

بِسْمِ اللَّهِ الرَّحْمَنِ الرَّحِيمِ

عن أبي هريرة رضي الله عنه قال قال رسول الله صلى الله عليه وسلم
إذا مات ابن آدم انقطع عمله إلا من ثلاث صدقة جارية أو علم ينتفع به أو ولد صالح يدعو له.

-رواه مسلم-1631

اللَّهُمَّ انفعني بما علمتني وعلمني ما ينفعني وارزقني علما تنفعني به

TABLE OF CONTENTS

TABLE OF CONTENTS.....	1
ACKNOWLEDGEMENTS.....	3
ABSTRACT.....	4
CHAPTER 0: INTRODUCTION.....	5
CHAPTER I: Basics.....	6
1.1 Stress.....	6
1.1.1 Introduction.....	6
1.1.2. Categorization of stresses.....	6
1.1.3. Stress intensity.....	8
1.1.4. Stress limits.....	8
1.2. Fatigue assessment of pressure vessels.....	9
1.2.1. Introduction.....	9
1.2.2. Stress-Life.....	10
1.2.2 Formalism and classification of multiaxial fatigue criteria.....	18
CHAPTER II: CONTRIBUTION.....	22
2.1. Analysis of Rankine cycle for the Tripoli-IPP 30 MW power plant.....	22
2.2. Software used for modeling and simulation.....	25
2.3. Files format.....	26
2.4. Designing CAD models for the vaporizer and for the drum.....	27
2.4. Meshing the CAD model.....	33
2.5. The solver Elmer.....	36
CHAPTER III: RESULTS AND DISCUSSION.....	37
3.1 CAD Model and Meshing of vaporizer and steam drum.....	37
3.2 Running the solver.....	37
3.3 Viewing results Paraview / VTK.....	38
3.4. Estimated number of constant amplitude fatigue cycles.....	47
3.5. Estimated fatigue safety factor caused by a multiaxial load.....	48
3.6. Probabilistic analysis of the number of fatigue cycles.....	50
3.7. Estimate of the number of cycles of elongation at constant amplitude.....	52
3.8. Estimated number of cycles due to displacement caused by a multiaxial load.....	53
3.9. Results of Fallo software.....	57
3.10. Results of FALSN software.....	58
3.11. Results of FALIN software.....	59
3.12. Discussions of all results.....	61

CHAPTER IV: CONCLUSION AND FUTURE WORK	62
BIBLIOGRAPHY	i
LIST OF FIGURE.....	ii
LIST OF TABLE.....	iii
GLOSSARY.....	iv
Annex	v
1. Annex 1: Water steam Diagram.....	v
2. Annex 2: Task of master thesis	vi
3. Annex 3: Time plan	vii
4. Appendix 4: The properties of the steam at the inlet of the turbine	viii
5. Annex 5: Blueprints of drum.....	ix
6. Annex 6: Physical properties of stainless steel 316L (Reference Materials Engineering- Mechanical Behavior Report 128)	x

ACKNOWLEDGEMENTS

عن أبي هريرة، عن النبي صلى الله عليه وسلم قال: "لا يشكر الله من لا يشكر الناس". رواه ابو داود. ورواه الترمذي عن أحمد بن محمد، عن ابن المبارك، عن الربيع بن مسلم وقال: صحيح.

The prophet Muhammad (peace be upon him) said: ***"Who doesn't thank a person (for something good), do not gives thanks to God"***.

First I want to thank Dr. Hamed Elkhatib, my professor at the Lebanese University for its support and assistance throughout the work. Also a big thanks to Dr. Abd El Fattah Khoder.

Then the great thanks go to my family , my father Khalid , Najat my mother and all my brothers and my sister.

Banan Elkerdi

Burj Akkar, Akkar/North Lebanon

18 October 2015

ABSTRACT

This thesis discusses the mechanical study of the incineration chamber and vaporizer (including climbing pipes) subjected to relatively high pressure, which may cause a relatively great mechanical stress leading to fatigue and damage and eventually break.

It is a study for upscaling the TEMO-IPP test plant in Ras Nhache, Batroun /Lebanon to a commercial 30 or 40 MW plant for a city like Tripoli/Lebanon.

The fracture mechanics and the study of fatigue phenomenon are relatively recent sciences that saw the bulk of their development in the 20th century. The issue of those fields of mechanics is the same: it is to predict the behavior of structures up to their ruin, as much as possible to avoid the dangers and high costs introduced by fatigue and breakage.

Theoretically, several methods exist to estimate the number of cycles before damage, in this study we use several software (Fallo, FALLIN, FALLPR, FALLSIN) specialized in the estimate that are combined together to predict the fewest estimated cycle .

Keywords: multiaxial fatigue, rupture, Rankine cycle, crack propagation, damage, free software, open source.

CHAPTER 0: INTRODUCTION

This thesis discusses the mechanical study of the incineration chamber and vaporizer (including climbing pipes) subjected to relatively high pressure, which may cause a relatively great mechanical stress leading to fatigue and damage and eventually break.

It is a study for upscaling the TEMO-IPP test plant in Ras Nhache, Batroun /Lebanon to a commercial 30 or 40 MW plant for a city like Tripoli/Lebanon, see Appendix 3.

The fracture mechanics and the study of fatigue phenomenon are relatively recent sciences that saw the bulk of their development in the 20th century. The issue of those fields of mechanics is the same: it is to predict the behavior of structures up to their ruin, as much as possible to avoid the dangers and high costs introduced by fatigue and breakage.

Theoretically, several methods exist to estimate the number of cycles before damage, in this study we use several software (Fallo, FALLIN, FALLPR, FALLSIN) specialized in the estimate that are combined together to predict the fewest estimated cycle .

CHAPTER I: Basics

1.1 Stress

1.1.1 Introduction

Stress is a tensor quantity (neither a vector nor a scalar) that depends on the direction of applied load as well as on the plane it acts. Generally speaking, at a given plane there are both normal and shear stresses. However, there are planes within a structural component (that is being subjected to mechanical or thermal loads) that contain no shear stress. Such planes are called principal planes and the directions normal to those planes are called principal directions. The normal stresses (only stresses in those planes) are called principal stresses. For a general three-dimensional stress state there are always three principal planes along which the principal stresses act. In mathematical terms we can say that the problem of principal stresses is an eigenvalue problem, with the magnitudes of the principal stresses being the eigenvalues and their directions (normal to the planes on which they act) being the eigenvectors. Principal stress calculations form an essential activity for a general stress analysis problem.

1.1.2. Categorization of stresses

Stresses are generally characterized as (a) primary stress, (b) secondary stress, or (c) peak stress. In the following discussion, the primary stresses will be denoted by P, the secondary stress by Q and the peak stress by F. These nomenclatures also apply to the ASME Boiler and Pressure Vessel Code We will now define each of the three categories of stress.

a. Primary stress

Primary stress is any normal stress or a shear stress developed by the imposed loading which is necessary to satisfy equilibrium between external and internal loads. These stresses are not self-limiting. If primary stresses are increased such that yielding through net section occurs, subsequent increase in primary stress would be through strain hardening until failure or gross distortion occurs. Generally primary stresses result from an applied mechanical load, such as a pressure load. The concept of equilibrium is based on a monotonic load and a lower bound limit load. Primary stresses are those that can cause ductile rupture or a complete loss of load-carrying capability due to plastic collapse of the structure upon a single application of load. The

purpose of the Code limits on primary stress is to prevent gross plastic deformation and to provide a nominal factor of safety on the ductile burst pressure.

Primary stresses are further divided into three types: general primary membrane (P_m), local primary membrane (P_L), and primary bending (P_b).

b. Secondary stress

Secondary stress originates through the self-constraint of a structure. This must satisfy the imposed strain or displacement (continuity requirement) as opposed to being in equilibrium with the external load. Secondary stresses are self-limiting or self-equilibrating. The discontinuity conditions or thermal expansions are satisfied by local yielding and minor distortions. The major characteristic of the secondary stress is that it is a strain-controlled condition. Secondary stresses occur at structural discontinuities and can be caused by mechanical load or differential thermal expansion. The local stress concentrations are not considered for secondary stresses. There is no need for further dividing the secondary stress into membrane and bending categories. In terms of secondary stress we imply secondary membrane and bending in combination.

c. Peak stress

Peak stress is the highest stress in a region produced by a concentration (such as a notch or weld discontinuity) or by certain thermal stresses. Peak stresses do not cause significant distortion but may cause fatigue failure. Some examples of peak stresses include thermal stresses in a bimetallic interface, thermal shock stresses (or stresses due to rapid change in the temperature of the contained fluid), and stresses at a local structural discontinuity.

Within the context of local primary membrane stress, P_L , as well as secondary stress, Q , the discontinuity effects need not be elaborated. The structural discontinuity can be either gross or local. Gross structural discontinuity is a region where a source of stress and strain intensification affects a relatively large portion of the structure and has a significant effect on the overall stress or strain pattern. Some of the examples are head-to-shell and flange-to-shell junctions, nozzles, and junctions between shells of different diameters or thicknesses. Local structural discontinuity is a region where a source of stress or strain intensification affects a relatively small volume of material and does not have a significant effect on the overall stress or strain pattern or on the structure as a whole.

1.1.3. Stress intensity

Let us indicate the principal stresses by σ_1 , σ_2 , and σ_3 . Then we define the stress differences by:

$$S_{1,2} = \sigma_1 - \sigma_2; S_{2,3} = \sigma_2 - \sigma_3; S_{1,3} = \sigma_1 - \sigma_3;$$

The stress intensity, SI , is then the largest absolute value of the stress differences, or in other words:

$$SI = \max[|S_{1,2}|, |S_{2,3}|, |S_{1,3}|]$$

The computed stress intensity is then compared with the material allowable taking into consideration the nature of the loading. The material allowable is based on yield and ultimate strength of the material with an implied factor of safety. Within the context of pressure vessel design codes, the comparison of the allowable strength of the material is always done with respect to the stress intensities. This puts the comparison in terms of the appropriate failure theory either the maximum shear stress theory (Tresca criterion) or the maximum distortion energy theory (von Mises criterion).

1.1.4. Stress limits

The allowable stresses (or more correctly the stress intensities) in pressure vessel design codes such as the ASME Boiler and Pressure Vessel Code are not expressed in terms of the yield strength or the ultimate strength but instead as multiples of tabulated design value called the design stress intensity (denoted for example as S_m). This value is typically two-thirds of the yield strength of the material or for other cases one-third of the ultimate strength. Therefore we have a factor of safety of 1.5 or 3 in terms of yield strength or ultimate strength, respectively. It is the purpose of the design codes that these multiples of either the yield or the ultimate strength are never exceeded in design.

The pressure vessel design codes often make specific recommendations on the limits depending on the conditions (or situations) of design. One typical such classification is in terms of design, normal, and upset (levels A and B), emergency (level C), faulted (level D) and test loadings, and accordingly limits are set appropriately. These stress limits have been discussed in some detail in Chapter 3. As an example, for design conditions the limits for the general primary

membrane stress intensity, P_m , the local primary membrane stress intensity, P_L , and the combined membrane and bending stress intensity $P_m (P_L) + P_b$, are typically expressed as:

$$P_m \leq S_m$$

$$P_L \leq S_m$$

$$P_L + P_b \leq 1.5S_m$$

These limits are sometimes higher than the actual operating conditions. It is the intent of the design code that the limit on primary plus secondary stresses be applied to the actual operating conditions. For normal and upset conditions (sometimes indicated as levels A and B), the range of primary and secondary stresses, $P_L \leq P_b \leq Q$ is not allowed to exceed $3S_m$, or

$$|P_L + P_b + Q|_{range} \leq 3S_m$$

A word of caution is needed here. For example, a stress limit on some of the combination of stress categories such as $P_m(P_L) \leq P_b$, $P_L \leq Q$ needs to be carefully understood. The confusion arises because of the tendency to denote the stress intensity in a particular category by the symbol of that category, for example P is the stress intensity for the primary bending stress category. However $(P_L \leq P_b \leq Q)$ is not the sum of the individual components of primary membrane, primary bending and secondary stress intensities. It is in fact the stress intensity evaluated from the principal stresses after the stresses from each category have been added together in the appropriate manner (that is not by adding the stress intensities). The primary plus secondary stress limits are intended to prevent excessive plastic deformation leading to incremental collapse, and to validate the application of elastic analysis when performing the fatigue evaluation. The limits ensure that the cycling of a load range results in elastic response of the material, also referred to as shakedown (when the ratcheting stops)[3].

1.2. Fatigue assessment of pressure vessels

1.2.1. Introduction

All structures and mechanical components that are cyclically loaded can fail by fatigue. With limited input data, constant amplitude fatigue analysis is used to make a simple and quick estimate of the likely fatigue performance or durability.

There are three primary methods for estimating the fatigue resistance of components and structures. **Stress-Life** analysis assumes that the stresses always remain elastic even at the stress concentrators. Most of the life is consumed nucleating small microcracks. This is typical for long life situations (millions of cycles) where the fatigue resistance is controlled by nominal stresses and material strength. **Strain-Life** is used for situations where plastic deformation occurs around the stress concentrations.

An example would be in a structure that has one major load cycle every day. Both stress-life and strain-life provide an estimate of how long it will take to form a crack about 1mm long.

Crack growth analysis is then used to estimate how long it will take to grow a crack to final fracture. Fatigue of welds requires special considerations because of their complex shape and loading.

1.2.2. Stress-Life

The stress life method is the classical method for fatigue analysis of metals and has its origins in the work of Wöhler in 1850. Stresses in the structure or component are compared to the fatigue limit of the material. The basis of the method is the materials S-N curve which is obtained by testing small laboratory specimens until failure.

a. Material Properties

Historically, these tests have been conducted in rotating bending. Today, it is often common to find test data for axial loading as well.

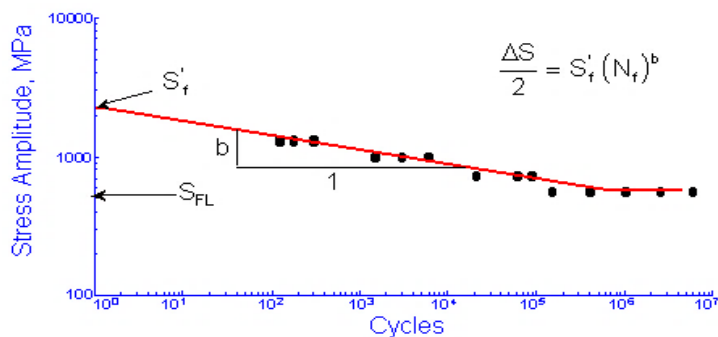


Figure 1: STRESS AMPLITUDE IN FUNCTION OF NUMBER OF CYCLES

The fatigue limit, S_{FL} , is the stress below which failures do not occur in the laboratory. Wöhler called this a safe stress level for design. Today we know that failures will occur below the safe

stress level but it will take a very large number of cycles, longer than the 10^6 or 10^7 cycles used in normal fatigue testing. The finite life portion of the curve is fit to a power function relating the stress amplitude, $\Delta S/2$, and fatigue life in cycles, N_f . Some people use reversals, $2N_f$, instead of cycles for plotting fatigue data. There are 2 reversals in one cycle. The intercept at 1 cycle, S'_f , and slope, b , are taken as material constants.

Many times the fatigue behavior of a material is unknown and must be estimated from the tensile properties. There is a strong correlation between fatigue strength and tensile strength [4].

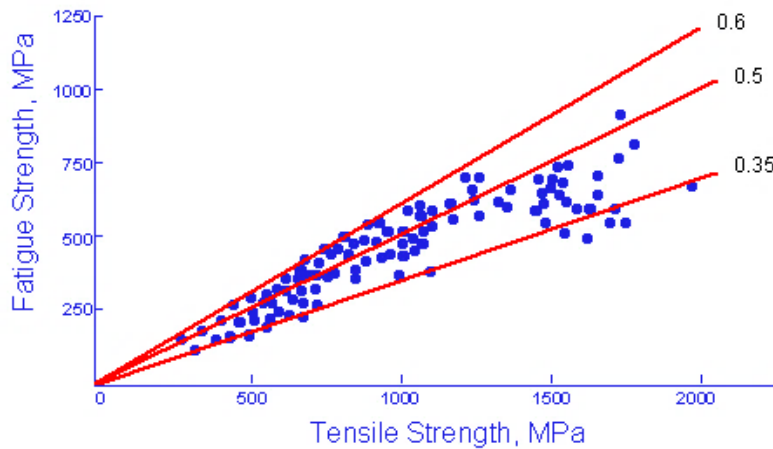


Figure 2:FATIGUE STRENGTH IN FUNCTION OF TENSILE STRENGTH

The fatigue limit is approximated as one half of the tensile strength.

$$S_{FL} = 0.5S_u$$

Many metal alloys are heat treatable and the hardness rather than the tensile strength are known. Another well-known approximation, with just as much scatter as shown above, is that the tensile strength, in English units of ksi, is approximately one half of the Brinell hardness, BHN. Combining these two approximations provides an estimate of the fatigue strength from the hardness.

$$S_{FL} = 0.25(BHN)$$

It has been observed that the fatigue strength at 1000 cycles is approximately $0.9 S_u$. This gives two points on the SN curve, both in terms of hardness that can be used to estimate the entire SN curve.

$$S_a = \frac{\Delta S}{2} = 1.62 S_u (N_f)^{-0.085}$$

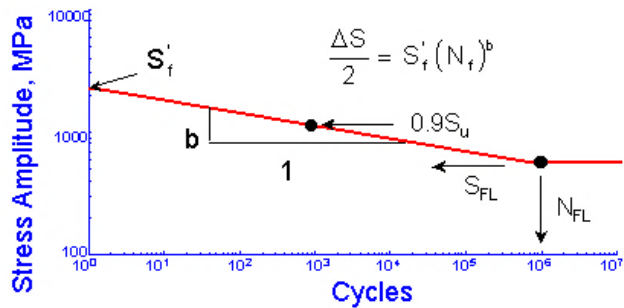


Figure 3: CALCULATION OF S_u AND S_{fl} FROM THE CURVE

Four material parameters are used to describe the materials stress life curve, S'_f , b , S_{FL} and N_{FL} , only three of which are independent. Leaving any one of the parameters blank will result in the fourth one being directly computed. If all four are entered, S_{FL} will be ignored.

b. Modifying Factors

Materials, as they are tested, are always in a different condition (surface finish, residual stress, etc.) from the materials as they are actually used. An important part of the analysis is to "correct" the basic materials data to obtain an estimate of the fatigue limit of the material in the component or structure of interest. Fatigue cracks usually nucleate on the surface so that the condition of the surface plays a major role in the fatigue resistance of a component. Test specimens are polished to eliminate the effects of surface finish. The degree of surface damage depends not only on the processing but also on the strength of the material. Higher strength materials are more susceptible to surface damage. To account for this in the analysis the

material fatigue limit is reduced by a surface finish factor, k_{SF} .

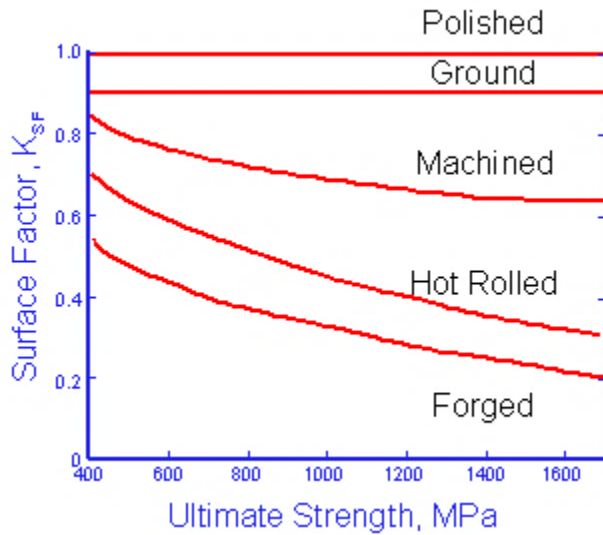


Figure 4: SURFACE FACTOR IN FUNCTION OF THE ULTIMATE STRENGTH

The original data for constructing this curve is shown below. The factors tend to provide conservative estimates for fatigue lives [5].

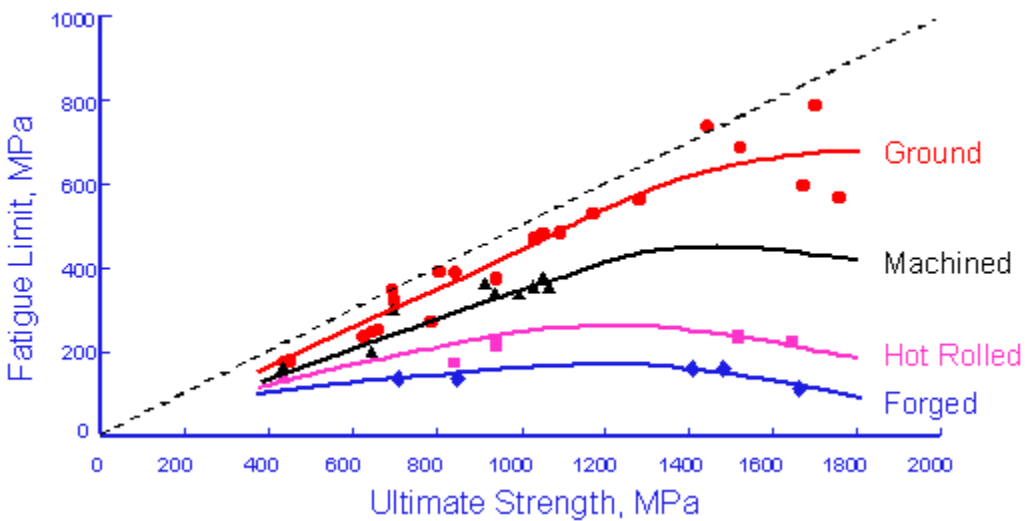


Figure 5: FATIGUE LIMIT IN FUNCTION OF THE ULTIMATE STRENGTH

These data are fit to a simple power function to obtain an estimate of the surface factor for any hardness steel.

$$k_{SF} = \alpha S_u^\beta$$

	A	β
Ground	1.58	-0.085
Machined	4.51	-0.265
Hot Rolled	57.7	-0.718
Forged	272	-0.995

Table 1: THE VALUES OF A AND BETTA

Fatigue limits have historically been determined from small specimens, 6 mm in diameter, tested in rotating bending. High strength materials tested in tension tend to have lower fatigue limits. An empirical load factor, k_L , is introduced for other types of loading.

	k_L
Tension, $S_u \leq 1500$ MPa	0.92
Tension, $S_u > 1500$ MPa	1.0
Bending	1.0
Torsion	0.58

Table 2: THE VALUES OF k_L

Experiments show that smaller components tend to have higher fatigue limits than larger ones. This is accommodated in the analysis by introducing a size factor, k_{size} . Some people call this a gradient factor. One of the most widely used corrections is based on the diameter of a bar.

$$k_{size} = \left(\frac{d}{7.62} \right)^{-0.1133} \quad 3 \leq d \leq 50$$

One of the problems associated with this simple approximation is what to do when the section is not round. This problem is overcome by defining an effective diameter. The volume of material subjected to 95% of the maximum stress in any shaped cross section is equated to a round bar of the same highly stressed volume. When these volumes are equated, the length canceled and the ratio becomes one of the relative areas. If we define the cross sectional area

of a non-circular section subjected to 95% of the maximum stress as $A_{0.95}$, then the effective diameter is given by

$$d = \sqrt{\frac{A_{0.95}}{0.077}}$$

Once these correction factors are determined, the fatigue limit of the machine component in the condition that it is being used in can be evaluated from the standard test specimen.

$$S_{FL}(\text{component}) = S_{FL}(\text{material}) \cdot k_{SF} \cdot k_L \cdot k_{size}$$

These generalized empirical factors have the greatest confidence when applied to steel because they were all derived from an extensive database on steel accumulated from over 100 years of testing. The figures above have shown considerable scatter in the test data so that the factors must be regarded as approximate and are no substitute for actual test data for a critical application. That said, they do provide a good first approximation when no test data is available.

c. Stress Concentrations

Stress concentrations are one of the most important factors affecting the fatigue life of any component or structure. These stress concentrations may be intentional in the design or unintentional such as deep machining marks or other processing related flaws. It seems reasonable to directly compare the maximum stress at a stress concentration to the estimated fatigue limit for that component [6].

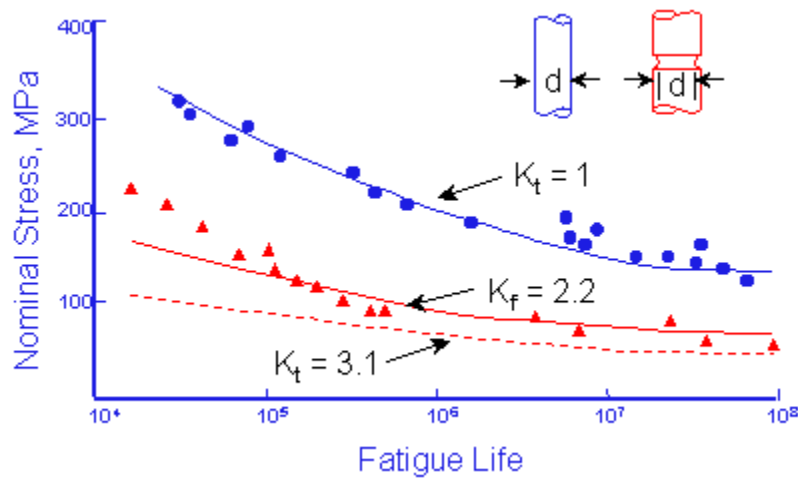


Figure 6: NOMINAL STRESS AND FATIGUE LIFE

Test data for an unnotched bar, such as the one above pictured in blue, are plotted as blue circles. This geometry has a stress concentration factor, K_t , equal to 1. The red dashed line represents estimated data for a geometry that has a stress concentration factor of 3.1, such as the notched bar pictured in red. The presence of the notch reduces the allowable nominal stress amplitude at any fatigue life by a factor equal to K_t . Notice that all of the actual test data, red triangles, lie above this estimate. This is because the effective stress concentration in fatigue is less than that predicted by the stress concentration factor, K_t . This effective stress concentration factor is called the fatigue notch factor, K_f . The variation between K_f and K_t is dependant on the size of the notch and strength of the material. A material that is very sensitive to notches will have K_f equal to K_t . If the material is very insensitive to notches, K_f will be close to 1. A notch sensitivity factor, q , is introduced to quantify this sensitivity [7].

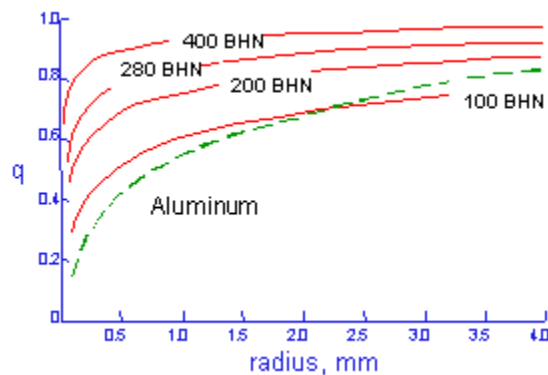


Figure 7: THE SENSITIVITY FACTOR IN FUNCTION OF RADIUS

Smaller radii are less effective in fatigue than larger ones. Fatigue notch factors can be computed from K_t and q .

$$K_f = 1 + (K_t - 1)q$$

Peterson fit the available test data for steel and aluminum to obtain an expression for K_f in terms of ultimate strength, S_u , and notch radius, ρ in mm.

$$K_f = 1 + \frac{K_t - 1}{1 + 0.025 \left(\frac{2070 \text{ MPa}}{S_u} \right)^{1.8}} \quad \text{for steel}$$

$$K_f = 1 + \frac{K_t - 1}{1 + \frac{0.5 \text{ mm}}{\rho}} \quad \text{for aluminum}$$

d. Mean Stresses

Tensile mean stresses are known to reduce the fatigue strength of a component. Compressive mean stresses increase the performance and are frequently used to increase the fatigue strength of a manufactured part. The most common method for accounting for mean stresses is the Goodman Diagram. It was first proposed in 1890. Goodman writes "... Whether the assumptions of the theory are justifiable or not.... We adopt it simply because it is the easiest to use, and for all practical purposes, represents Wohler's data." The fatigue limit for zero mean stress is plotted on one axis and the ultimate strength on the other.

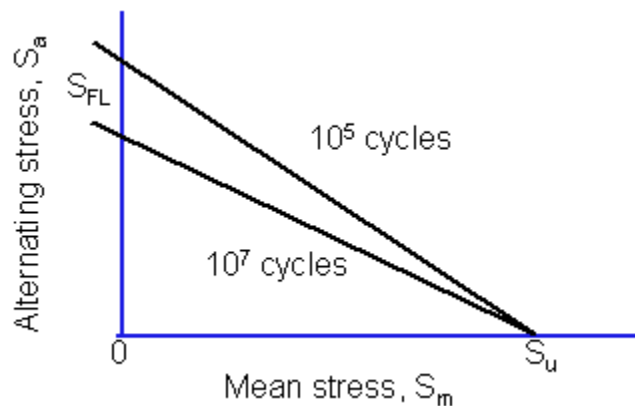


Figure 8: ALTERNATING STRESS IN FUNCTION OF MEAN STRESS

The diagram can be described by

$$\frac{S_a}{S_{FL}} + \frac{S_m}{S_u} = \frac{1}{n}$$

Stress concentration effects can be directly included in the Goodman diagram.

$$\frac{K_f S_a}{S_{FL}} + \frac{K_f S_m}{S_u} = \frac{1}{n}$$

For finite lives, an equivalent completely reversed stress, S_{eq} , is computed and compared with the component SN curve.

$$S_{eq} = \frac{S_a}{1 - \frac{K_f \cdot S_m}{S_u}}$$

Here K_f is used to modify the mean stress but not the stress amplitude because stress concentration effects are already included in the component SN curve.

1.2.2 Formalism and classification of multiaxial fatigue criteria

A literature review has identified 37 criteria of fatigue. The set of criteria are divided into three distinct approaches that differ in their concept.

The first approach, called empirical, includes criteria the formalism derived from experimental results obtained for a type of multiaxial stress and equipment donated.

The second approach is called the comprehensive approach. It brings together the criteria which involve invariants of the stress tensor and its diverter. These amounts representing all the constraints in a scalar give the criteria implementing them is comprehensive. Certain criteria define quantities related to the set of possible physical planes passing through the point at which the study is fatigue then driving into a root mean in general. The latter provides as the criteria based on this principle a full appearance.

The third approach, critical type of plan, collates criteria the formalism is based on research of a critical physical. Damage to material fatigue at the point where the stress is known, is related to their action on the plane in question.

Of these three approaches, subgroups differentiate formalisms criteria. We distinguish the macroscopic criteria involving evaluated constraints on a macroscopic scale. The choice of the

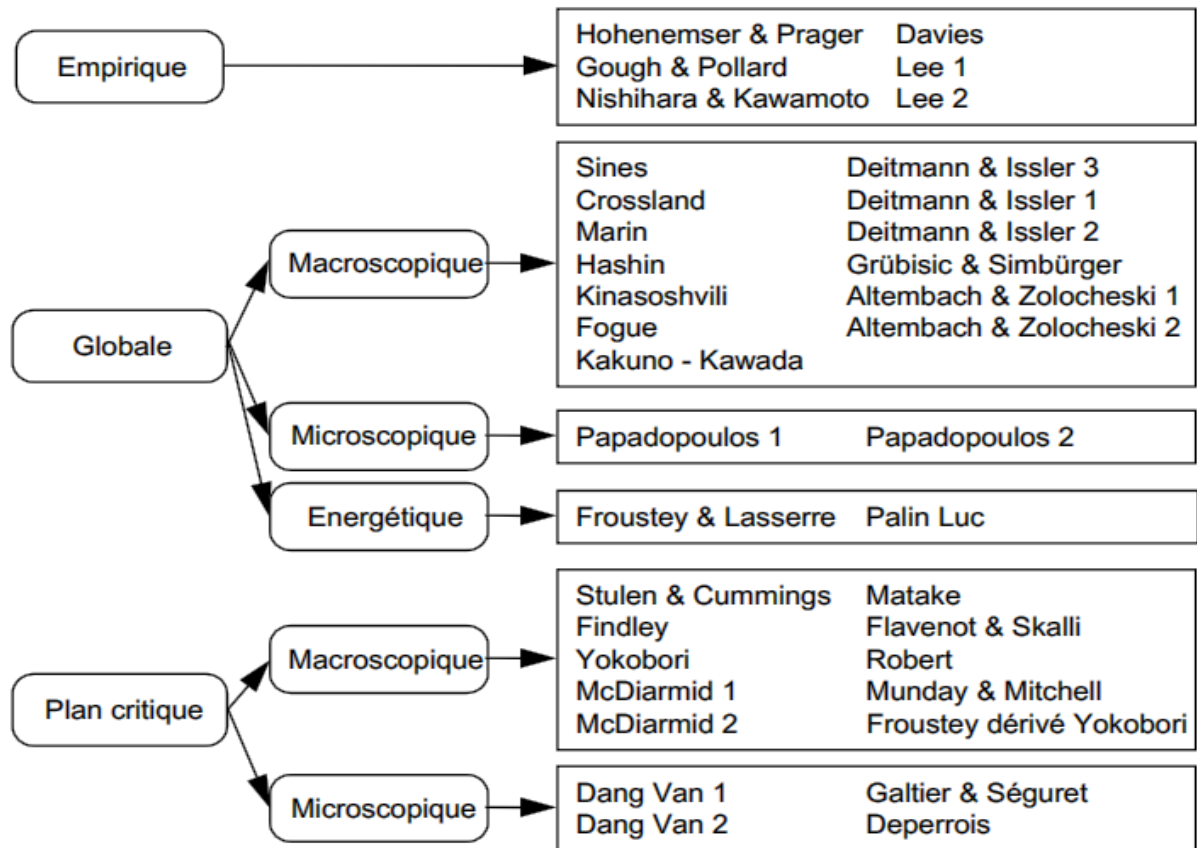


Figure 9: MULTIAXIAL FATIGUE CRITERIA AND THEIR CLASSIFICATION

terms involved in defining constraints such criteria is justified by their author. Other criteria are based on the behavior of the material on a microscopic scale . They expressed though their microscopic Final formalism uses macroscopic

Figure 9 summarizes all the multi-axial fatigue criteria listed in literature and their classification .

The empirical approach criteria

This category includes six criteria . They come from experimental results generally obtained for a type of multi-axial stress determined. It's about usually tension-torsion or bending - torsion , usually in phase. We found among these older models criteria , those of Hohenemser & Prager and Gough & Pollard that were developed in 1933 and 1935 respectively . The latest models proposed by Lee dating from 1980 [4,5] and 1989 [6,7].

The Hohenemser & Prager criterion

The Hohenemser & Prager criterion is the first criterion identified . Established in 1933, it was obtained from tension-torsion tests where the shear is variable and the normal stress σ_m traction is static;

$$E_{HP} = \left(\frac{\tau_a}{\tau_{-1}} \right)^2 + \frac{\sigma_m}{R_m}$$

The criterion Gough & Pollard

From many bending - torsion testing in phase , Gough & Pollard defined in 1935 two formulations that represent , in the reference related to the amplitudes of the normal bending stress and shear stress , ellipses . The first expression given below is for ductils materials

$$E_{GP} = \left(\frac{f_a}{f_{-1}} \right)^2 + \left(\frac{\tau_a}{\tau_{-1}} \right)^2$$

The second formulation involves the same quantities as before, but which is adapted to fragile materials. Fatigue function is as follows :

$$E_{GP} = \left(\frac{\tau_a}{\tau_{-1}} \right)^2 + \left(\frac{f_{-1}}{\tau_{-1}} - 1 \right) \left(\frac{f_a}{f_{-1}} \right)^2 + \left(2 - \frac{f_{-1}}{\tau_{-1}} \right) \left(\frac{f_a}{f_{-1}} \right)$$

Davies criterion

Davies, in 1935, adopted a formulation similar to that of Hohenemser & Prager . It only models the evolution of the amplitude of the allowable shear according to a normal static stress σ_m but the opposite , i.e. it observes the amplitude of the allowable normal stress bending as a function of static shear stress m_τ . He built from his observations the following modeling:

$$E_{DA} = \left(\frac{f_a}{f_{-1}} \right)^2 + \frac{\tau_m}{\tau_u}$$

The criterion of Nishihara & Kawamoto

In 1941, Nishihara & Kawamoto offer two models from their experimental findings that are distinguished by the value of the ratio of the endurance limit symmetrical alternating bending endurance limit and symmetrical alternate twist . Both models are written:

$$E_{NK} = \left(\frac{\tau_a}{\tau_{-1}} \right)^2 + \left(\frac{f_a}{f_{-1}} \right)^2 \quad \text{si } \frac{f_{-1}}{\tau_{-1}} \geq \sqrt{3}$$

$$E_{NK} = \left(\frac{\tau_a}{\tau_{-1}} \right)^2 + \frac{1}{2} \left(3 - \left(\frac{f_{-1}}{\tau_{-1}} \right)^2 \right) \frac{f_a}{f_{-1}} + \frac{1}{2} \left(\left(\frac{f_{-1}}{\tau_{-1}} \right)^2 - 1 \right) \left(\frac{f_a}{f_{-1}} \right)^2 \quad \text{si } \frac{f_{-1}}{\tau_{-1}} \leq \sqrt{3}$$

The criterion of Lee 1

More recently, in 1980, Lee offers a way out of modeling bending -torsion testing out phase. It introduces α -dependent phase shift ϕ between the two loads and defined by $\alpha = 2 (1 + \beta \sin \phi)$ where β is a constant related to the materials . The criterion is given by the following relationship

$$E_{LEE1} = f_a \left[1 + \left(\frac{\tau_a f_{-1}}{f_a \tau_{-1}} \right)^\alpha \right]^{1/\alpha}$$

The criterion of Lee 2

In 1989, Lee changed his first empirical criterion to add the influence of a average flexion. His last criterion involves an exponent n , between 1 and 2, is an empirical constant:

$$E_{LEE2} = \frac{E_{LEE1}}{\left[1 - \left(\frac{\sigma_m}{R_m} \right)^n \right]} = \frac{f_a \left[1 + \left(\frac{\tau_a f_{-1}}{f_a \tau_{-1}} \right)^\alpha \right]^{1/\alpha}}{\left[1 - \left(\frac{\sigma_m}{R_m} \right)^n \right]}$$

CHAPTER II: CONTRIBUTION

2.1. Analysis of Rankine cycle for the Tripoli-IPP 30 MW power plant

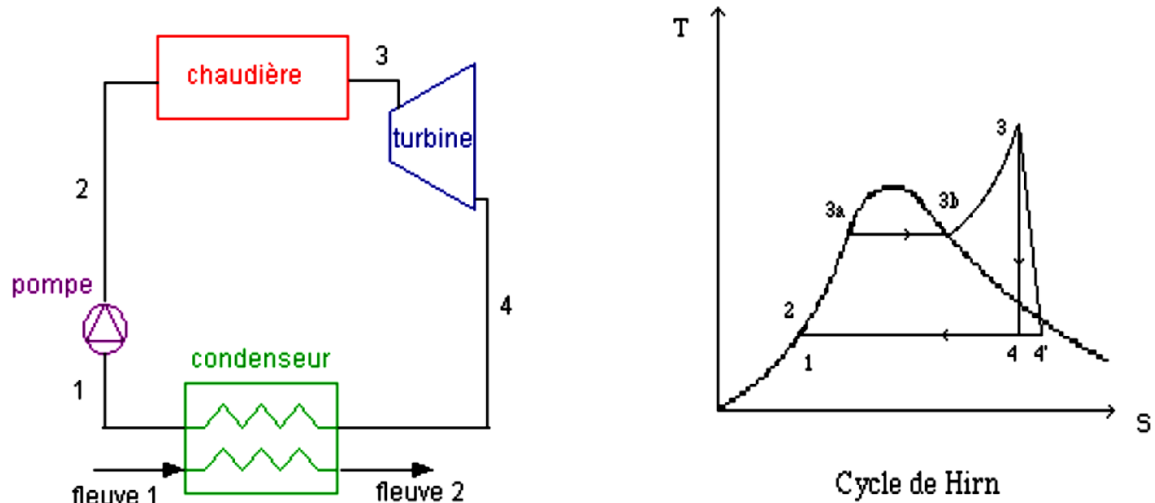


Figure 10: RANKINE CYCLE AND HIRN CYCLE

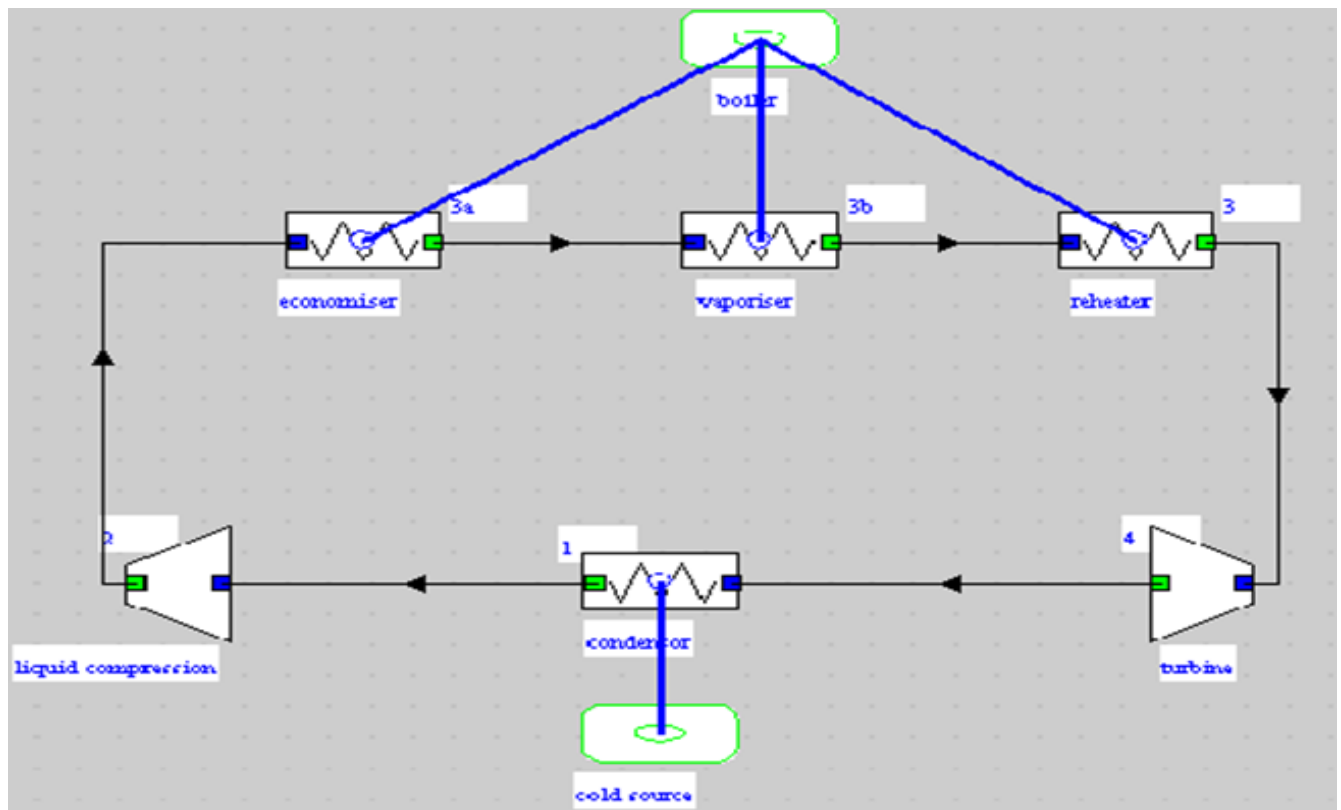


Figure 11: RANKINE CYCLE MODELISATION IN THERMOPTIM

In point 1, a 1 kg / s water flow is in the liquid state at a temperature of about 20 ° C, under low pressure (0.023 bars).

A Pump puts that water isentropically with an efficiency equal to 1 to a pressure of 165 bar (Point 2).

The pressurized water is then heated at constant pressure in a flame boiler (waste).

The warm up has three stages:

- Heating the liquid in the economizer, 20 ° C to about 355 ° C, initial boiling point temperature 165 bar: evolution (2-3a) on the entropy diagram
- Constant temperature 355 ° C vaporization in the vaporizer: evolution (3a -3b)
- Overheating of 355 ° C to 560 ° C in the superheater: evolution (3b -3).

The steam is then expanded in a turbine isentropically with an efficiency of 0.85, until the 0,023 bar pressure change (3-4).

The liquid-vapor mixture is then condensed to the liquid state in a condenser exchanger between the ring and the cold source, for example water of a river. The cycle is closed.

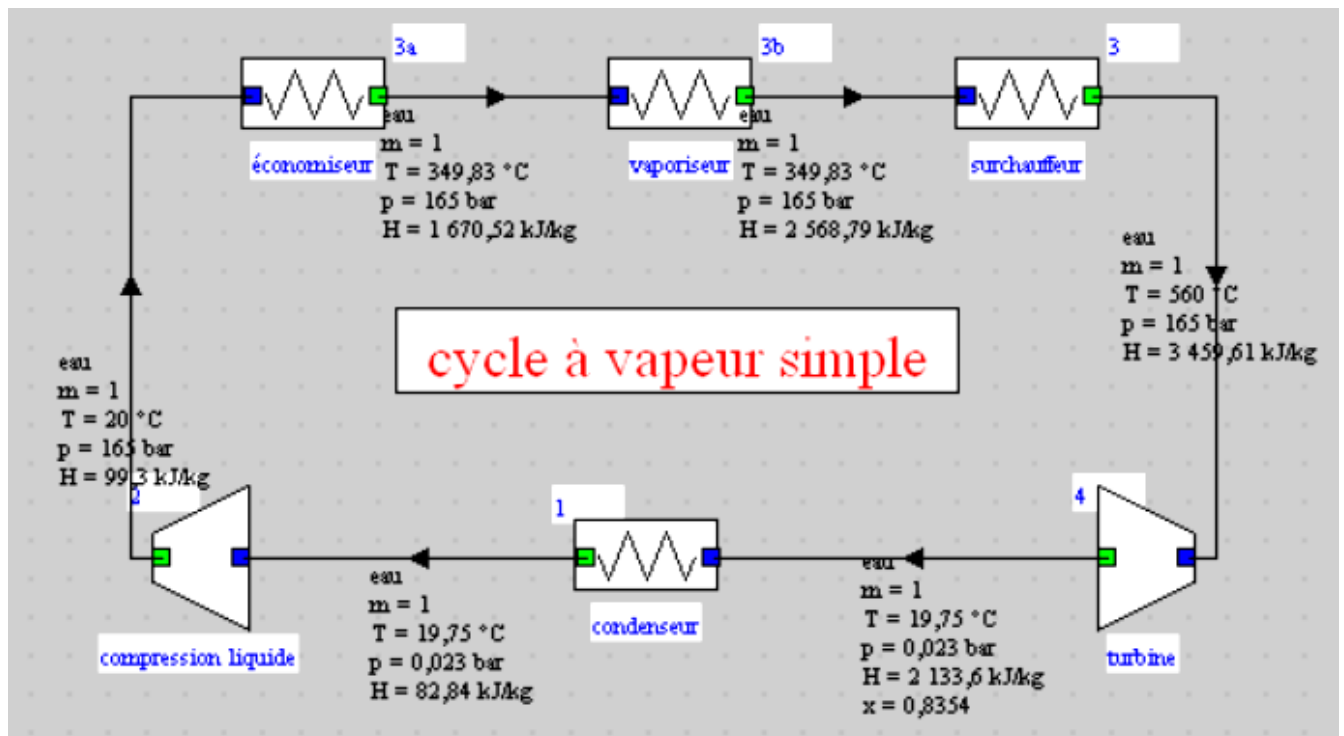


Figure 12: VALUES OF TEMPERATURE AND PRESSURE OBTAINED BY THERMOPTIM

nom du point	température T (°C)	pression P	enthalpie h	entropie s	volume v
1	19,74562	0,023	82,83661	0,292821	0,00100167
2	19,99591	165	99,29743	0,292809	0,000994375
3a	349,82707	165	1 670,51999	3,77803	0,00173903
3b	349,82707	165	2 568,79443	5,22016	0,00883163
3	560	165	3 459,61452	6,49548	0,0209757
4	19,74562	0,023	2 133,6008	7,29439	49,04255

Table 3: Results obtained using THERMOPTIM

The Rankine cycle is important to calculate the thermal efficiency (30 %), while for a turbine that produces 30 MW of electricity we need a thermal power of 90 MW.

And according to the thermal power the value of the combustion chamber is dimensioned.

The volume of the combustion chamber adapted from a study [0].

The volume is 7,500 cu ft (212 cubic meters) spread over 4 m long, 4 m wide and 12 m high.

2.2. Software used for modeling and simulation

Many software packages are used in this study, and we adopted different strategies to achieve this work (concerning the design, the meshing, the solving and the visualization for results).

In the schematic shown below we describe this chain of tools used. The tools adopted in this thesis are colored in green and these colored in red were tried also during a long time in this master thesis but finally were not adopted, because they are not Free tools (without licence), and sometimes because there is so limited and can't support a big value of data.

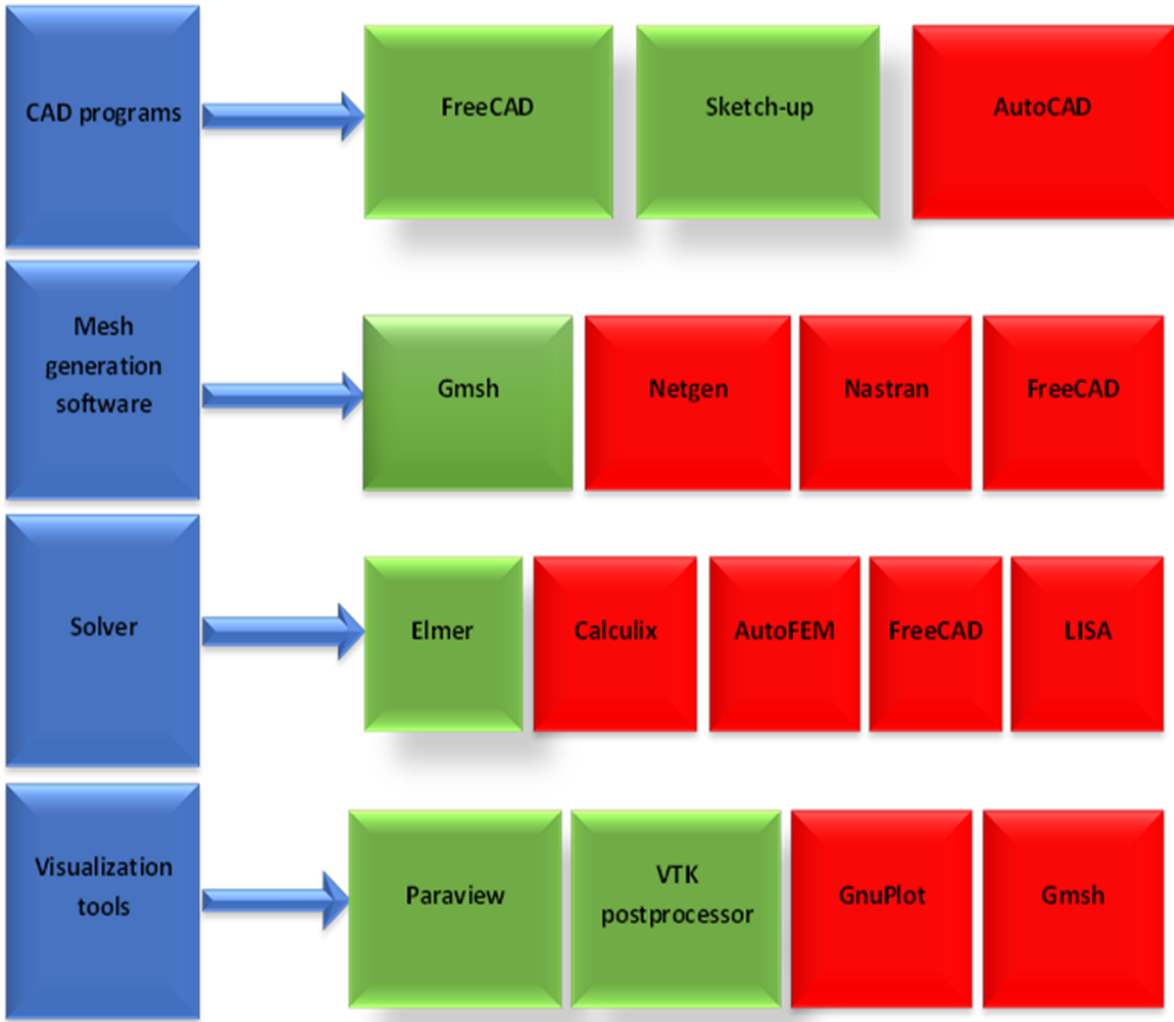


Figure 13: THE FREE AND OPEN SOURCE TOOLS USED IN THE STUDY

2.3. Files format

One of the difficulties was the problem of transition from one tool to another.

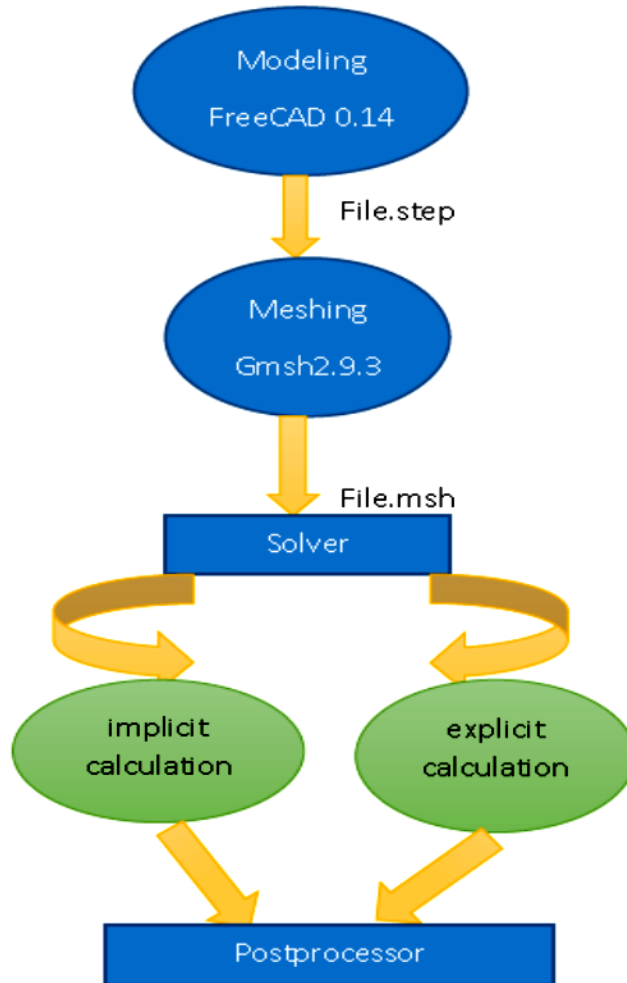


Figure 14: THE FORMAT OF FILES

2.4. Designing CAD models for the vaporizer and for the drum

Several forms exist in the market, which are shown in the figure 2.4.1. We have adopted the simplest form to facilitate the industry process (Figure 2.4.2 and 2.4.3), especially manufacturing of boiler will be local.

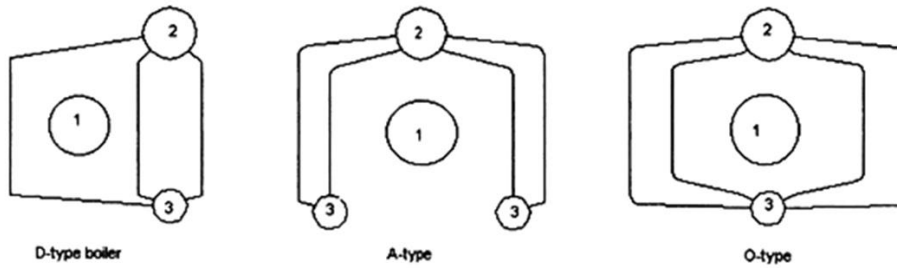


Figure 15: A-, D- and O-type boiler configurations. 1. Burner; 2. Steam drum; 3. mud drum

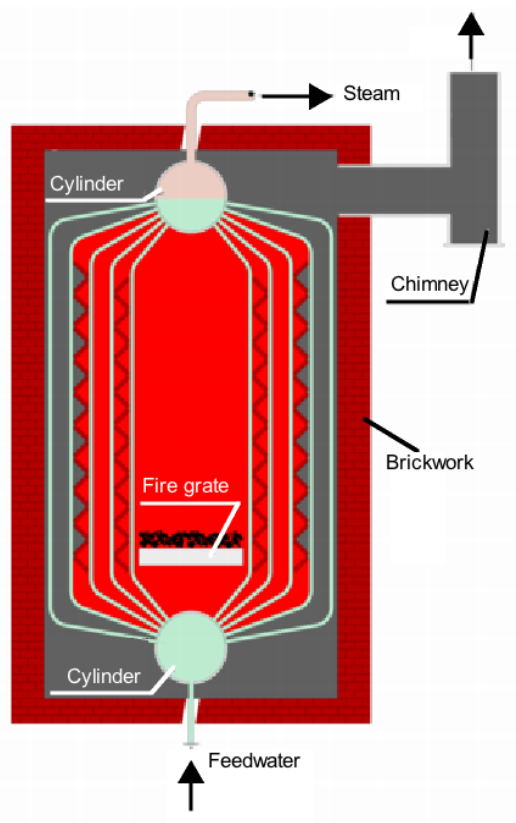


Figure 17: SCHEMATIC OF BOILER

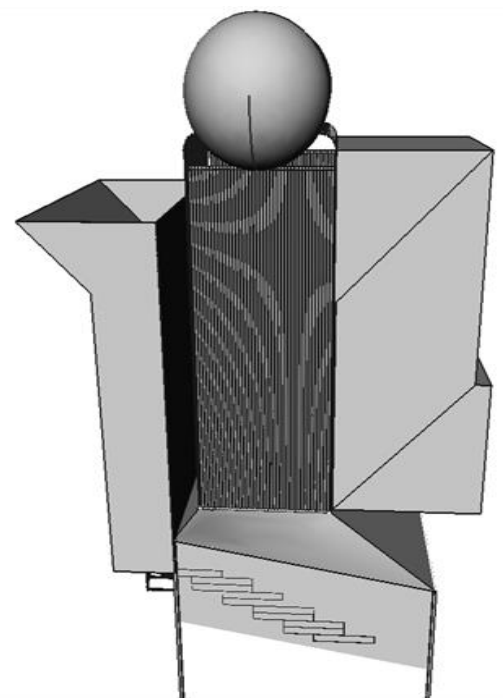


Figure 16: DESIGN IN FREECAD

The volume of the combustion chamber (including vaporizer) is adapted from the study shown in [12]. The volume is 7500 cu ft. (212 meter cube) distributed on 4 m length, 4 m width and 12 m height.

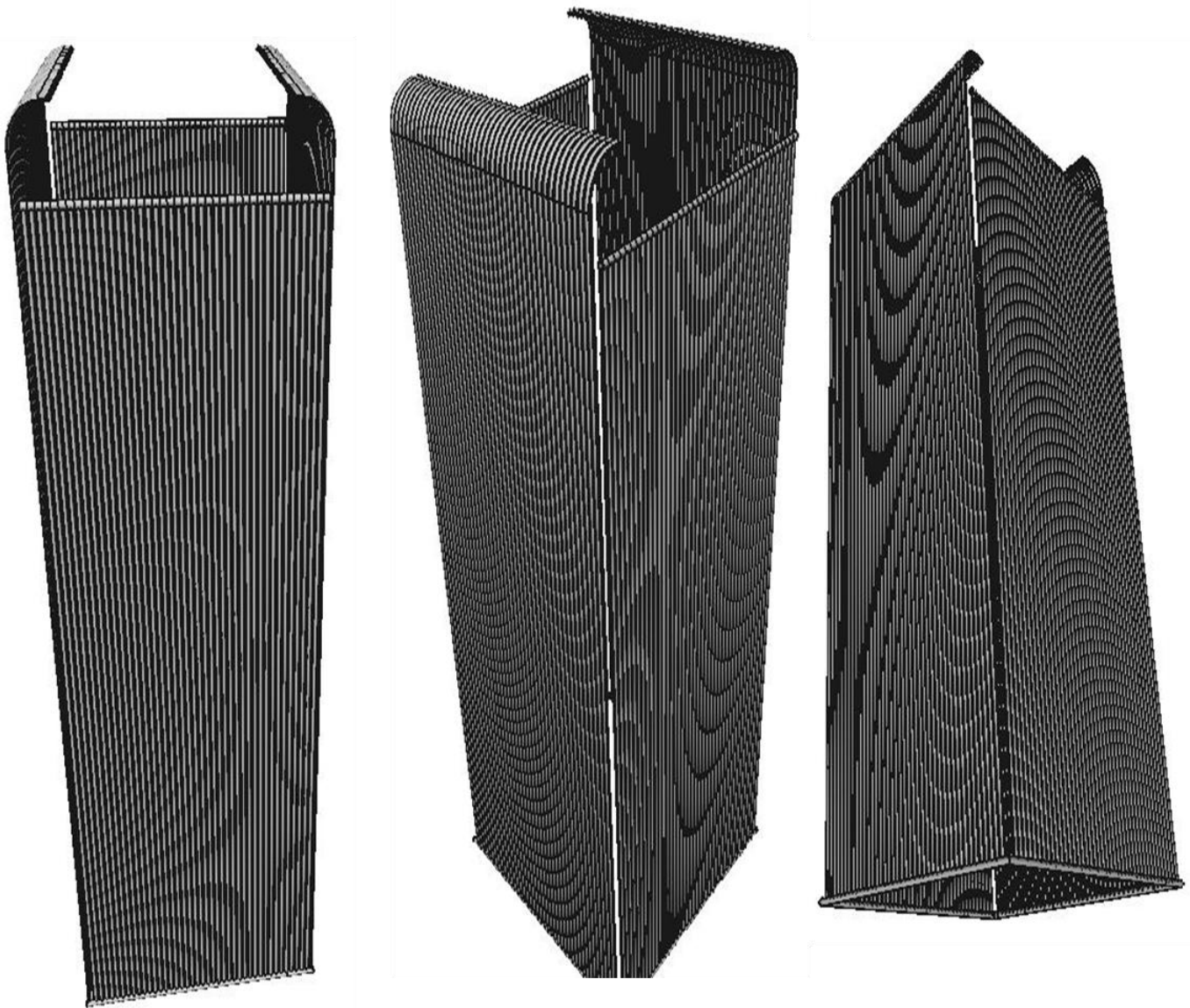


Figure 18: THE VAPORIZER IN FREECAD

• The properties of drum:

- Length: 32 ft. (10 m)
- Diameter: 7 ft. (2.1 m)
- Weight: 9200 pound (4173 kg)
- Capacity: 6600 gallon (24 983 l)

} (all this information are obtained from Annex 5)

- Thickness: 5 mm (this thickness is deduced from the browser in this site
<http://steelfinder.outokumpu.com/storage-tank/>)
- Material: Stainless steel 316L (physical properties of stainless steel 316L in Annex 6)

The screenshot displays the 'YOUR STORAGE TANK REQUIREMENTS' form on the website. The input fields are as follows:

- Temperature (°C): 260
- Height (m): 10
- Diameter (m): 2
- Density (specific): 0,5
- Steel grade: Supra 316L/4404
- Compare a Steel grade: Supra 316L/4404
- Design stress (MPa): 99
- Design stress (MPa): 99
- Joint factor: 1
- Joint factor: 1
- Plate width (mm): 2 000
- Corrosion allowance (mm): (empty)
- Plate width (mm): 2 000

The diagram shows a cross-section of a tank with two vertical walls. Each wall is composed of five horizontal plates, each labeled '5 mm'. The top and bottom of the tank are also labeled 'Supra 316L/4404'.

CALCULATION RESULT
 Material consumption Supra 316L/4404: **2 metric tons**
 Material consumption Supra 316L/4404: **2 metric tons**

Figure 19: Calculation of thickness via browser (chosen material is steel 316L)

← → C steelfinder.outokumpu.com/storage-tank/  

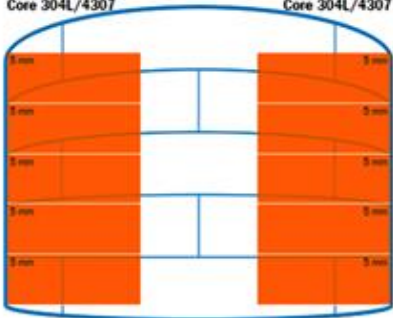
Help us make Steel Finder better!
 [Later](#) [never](#)

Storage tank shell thickness calculation tool based on the API650 and EN 14015 standards allows you to estimate material consumption for the cylindrical shell of a tank and to compare how steel grade affects material consumption. This tool can be used for estimation only. We are happy to discuss your requirements in more detail.

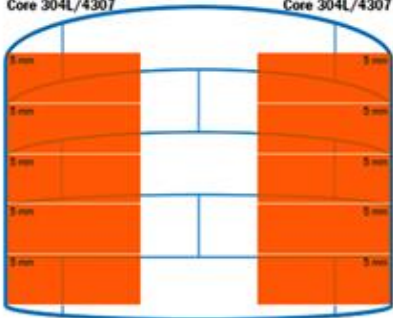
YOUR STORAGE TANK REQUIREMENTS

Temperature (°C) -40°C - 260°C	Height (m) 2m - 30m
<input type="text" value="20"/>	<input type="text" value="10"/>
Diameter (m) 2m - 60m	Density (specific) 0,5 - 3
<input type="text" value="2"/>	<input type="text" value="3,0"/>
Steel grade Core 304L/4307	Compare a Steel grade Core 304L/4307
Design stress (MPa) 145	Design stress (MPa) 145
Joint factor 1	Joint factor 1
Plate width (mm) 2 000	Corrosion allowance (mm) <input type="text"/>
<input type="button" value="Calculate"/>	Plate width (mm) <input type="text" value="2 000"/>

Core 304L/4307



Core 304L/4307



The picture above illustrates the number of plates and thickness by plate needed to build a tank with your specifications.

CALCULATION RESULT
 Material consumption Core 304L/4307: **2 metric tons**
 Material consumption Core 304L/4307: **2 metric tons**

Figure 20: Calculation of thickness via browser (chosen material is steel 304L)

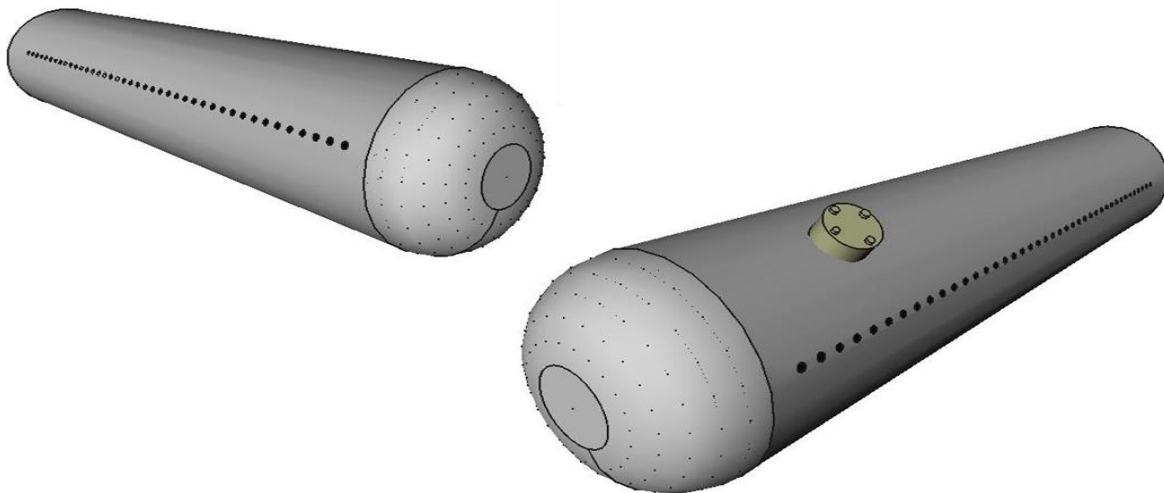


Figure 21: Design of Drum in FreeCAD

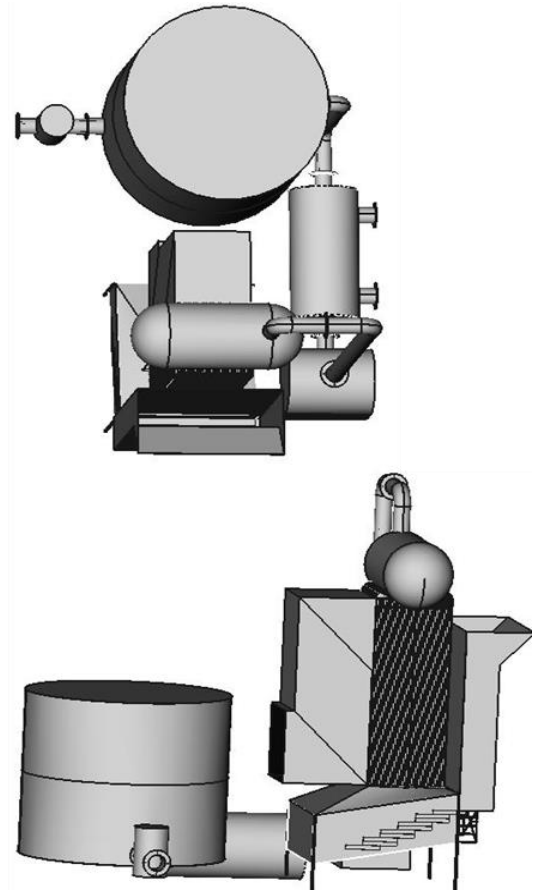
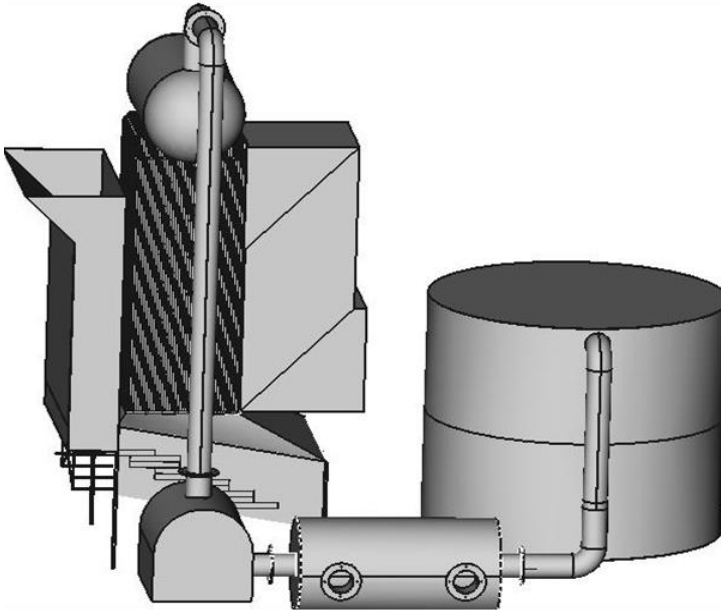


Figure 22: Group of all parts of a power plant in FreeCAD (boiler, drum, turbine, and condenser)

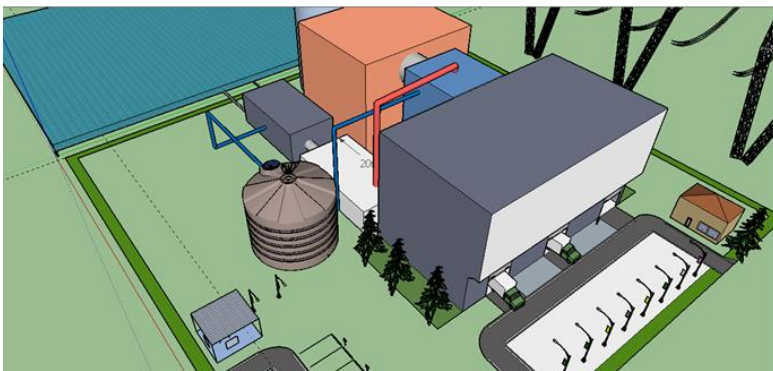
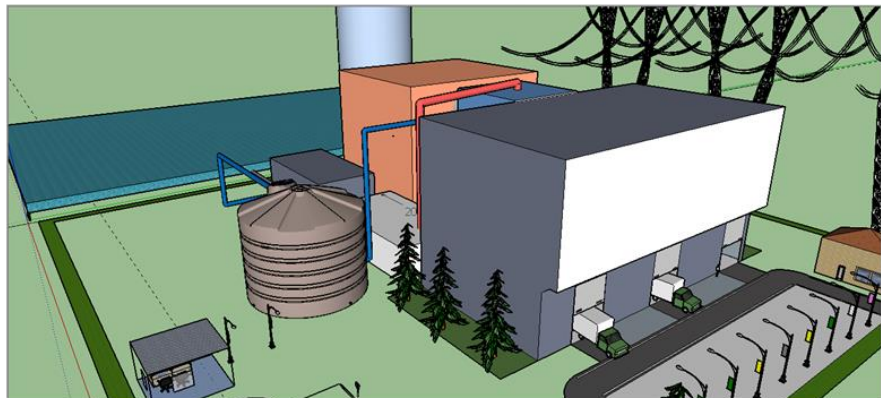
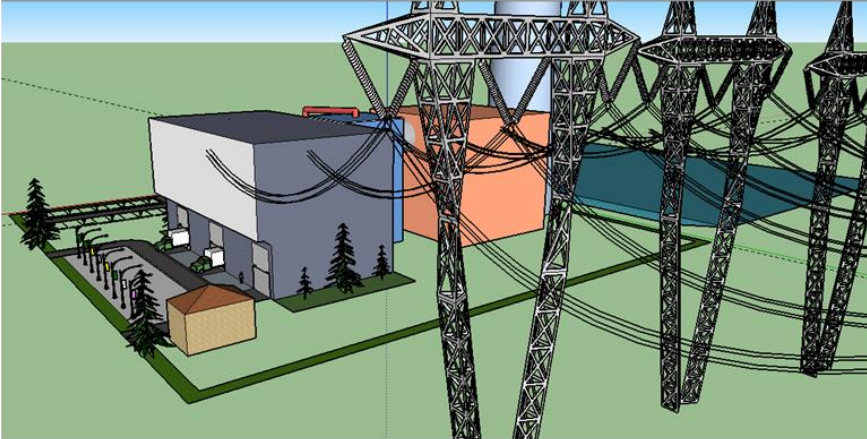
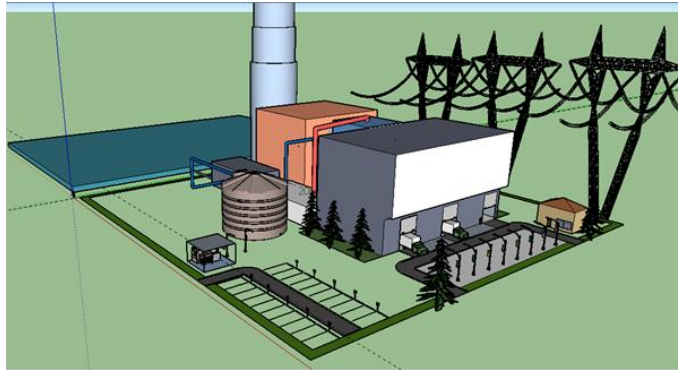


Figure 23: Design for of the incineration thermal power plant on a real ground using sketch-up (100 m ×100 m)

2.4. Meshing the CAD model

To mesh the CAD model we adopted first FreeCAD(FEM module), but we discovered that FreeCAD is unable to mesh our design entirely. FreeCAD is under construction and actually it can mesh only one element.

So we searched for other software to make the mesh and we found: Nastran, Netgen and Gmsh. All this tools are Free and open source.

We tried all this software and we found that the best is Gmsh because of the possibility of identifying the type of shape in FEM and its ability to mesh complex design in a time relativley short in comparaisn with the others.

Gmsh is built around four modules: geometry, mesh, solver and post-processing. Each module can be controlled either interactively using the GUI or using the scripting language.

The design of all four modules relies on a simple philosophy "be fast, light and user-friendly".

Fast: on a standard personal computer at any given point in time Gmsh should launch instantaneously, be able to generate a "larger than average" mesh (compared to the standards of the finite element community; say, one million tetrahedra in 2008) in less than a minute, and be able to visualize such a mesh together with associated post-processing datasets at interactive speeds.

Light: the memory footprint of the application should be minimal and the source code should be small enough so that a single developer can understand it. Installing or running the software should not depend on any non-widely available third-party software package.

User-friendly: the graphical user interface should be designed in such a way that a new user can create simple meshes in a matter of minutes. In addition, the code should be robust, portable, scriptable, extensible and thoroughly documented |all features contributing to a user-friendly experience.

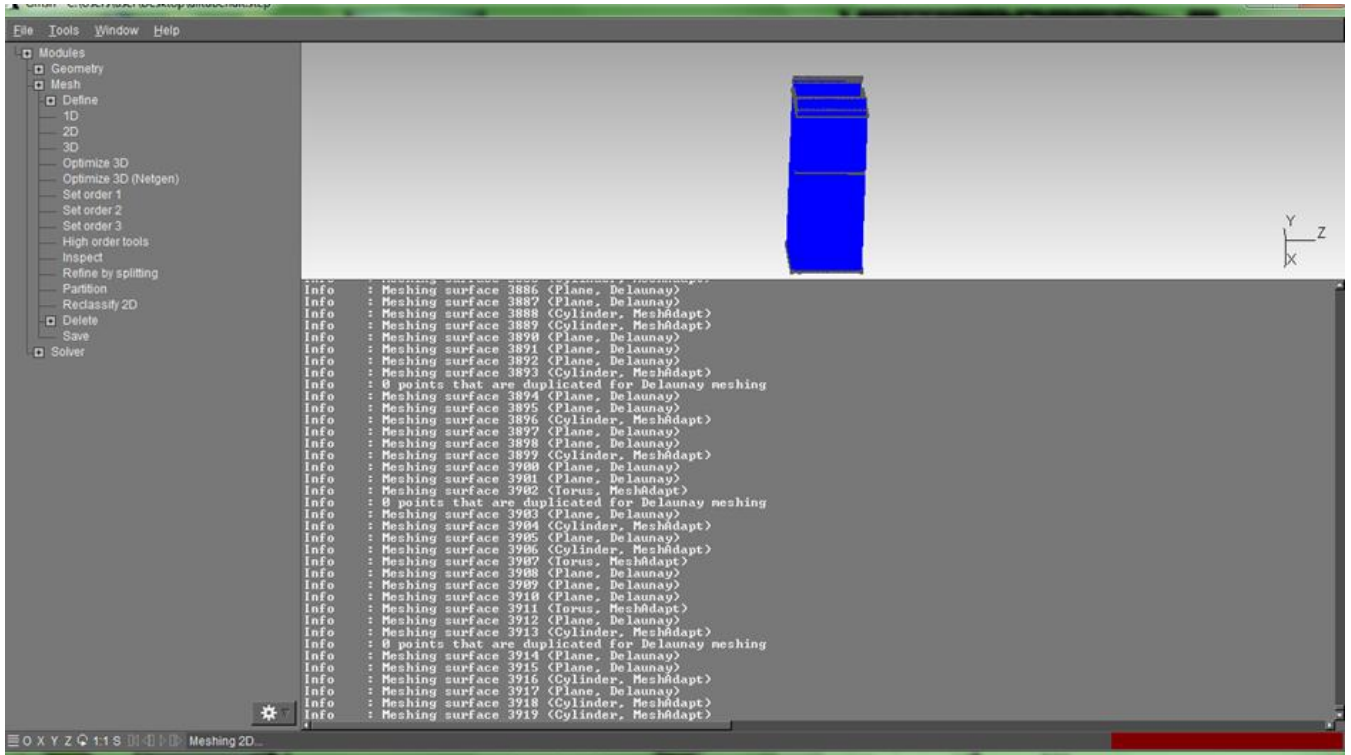


Figure 24: User Interface of Gmsh

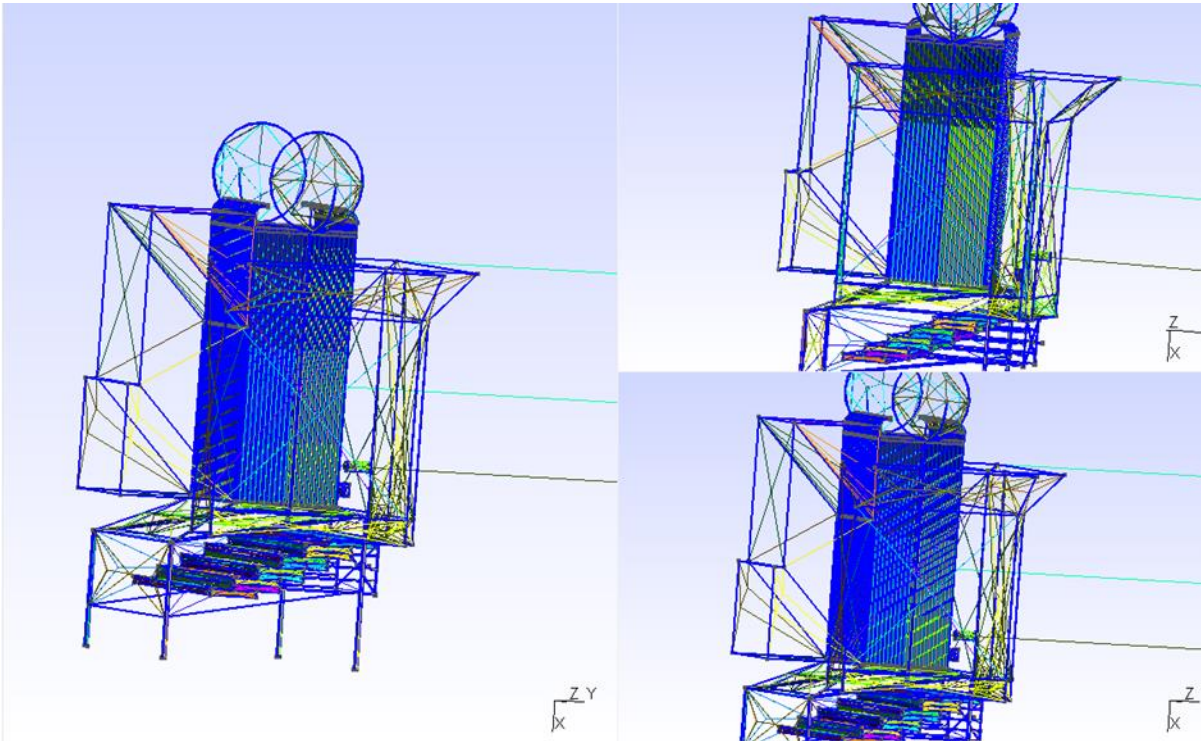


Figure 25: Mesh of the incinerator CAD model in Gmsh

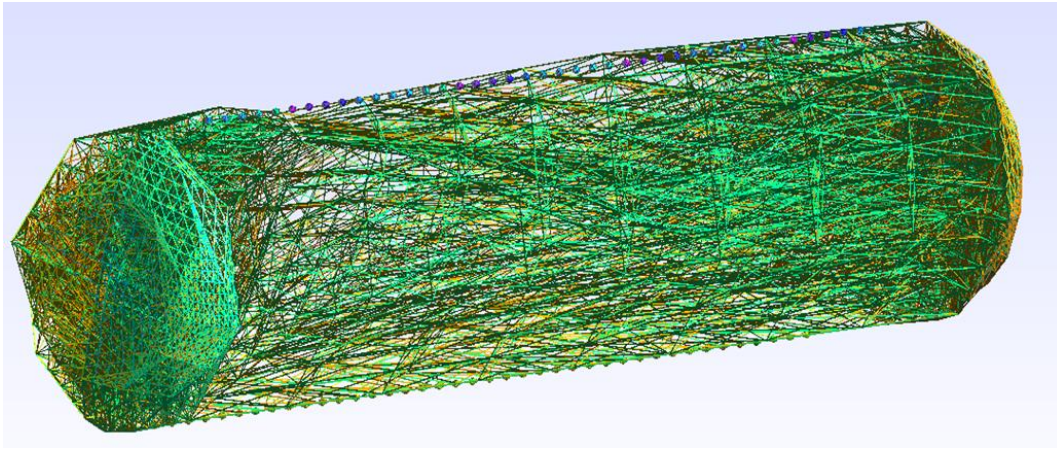


Figure 26: Mesh of the drum CAD model in Gmsh

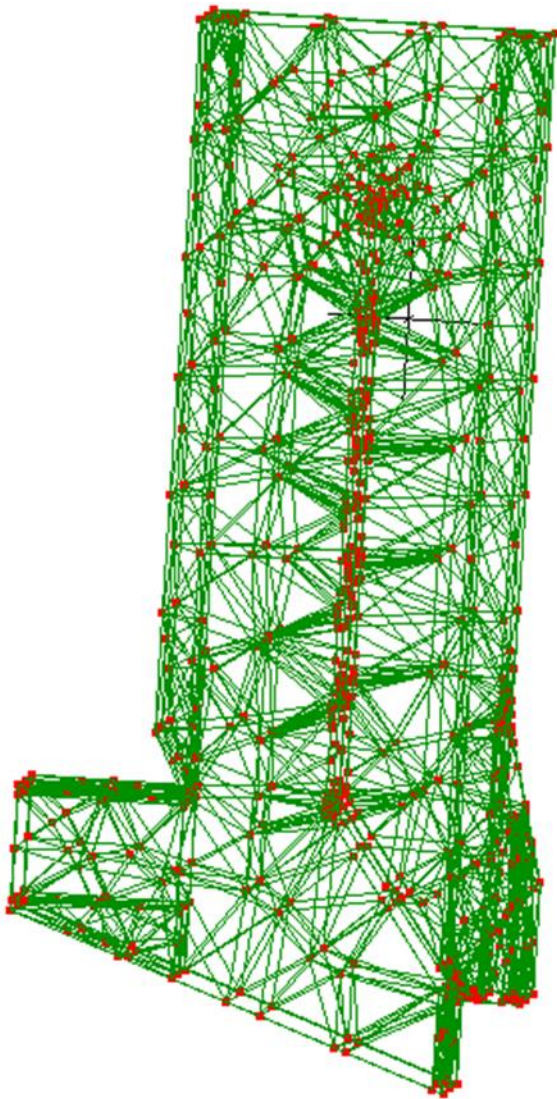


Figure 27: Mesh of the combustion chamber CAD model in Gmsh

2.5. The solver Elmer

Elmer is a combination of different software packages for the simulation of multiphysics problems using the Finite Element Method (FEM). Three of these software packages are: ElmerGUI, ElmerSolver, ElmerPost. Elmer is an open source software, released under the GNU General Public License (GPL).

Elmer can be used in two different ways:

- By using its Graphical User Interface (GUI). (A command text file can be generated after a GUI session).
- By using a command text file

Elmer has not good capabilities for geometry generation (CAD model) and meshing. Therefore, as a general procedure, the geometry and mesh should be imported into Elmer. It accepts different geometry and mesh formats. Among them, it accepts the GMSH mesh format.

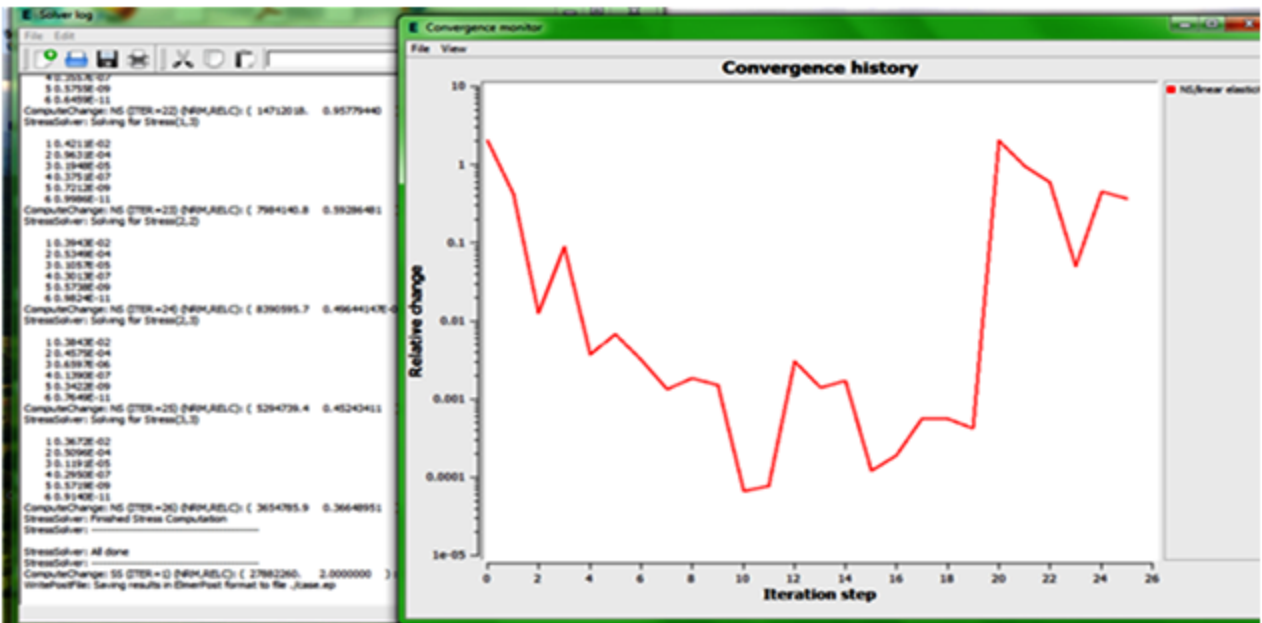


Figure 28: Convergence history window in ElmerSolver.

The convergence story appears during solving the partial differential equations (PDE) by the processor.

The vertex of the graph indicates that the processor solves the PDEs easily, whereas a peak indicates that the resolution of PDE faces difficulties in the system and it needs extra time.

CHAPTER III: RESULTS AND DISCUSSION

3.1 CAD Model and Meshing of vaporizer and steam drum

In this master thesis one of the important tasks is to determinate the location of the region exposed to a high stress. With Elmer we determinate the stress in the boiler.

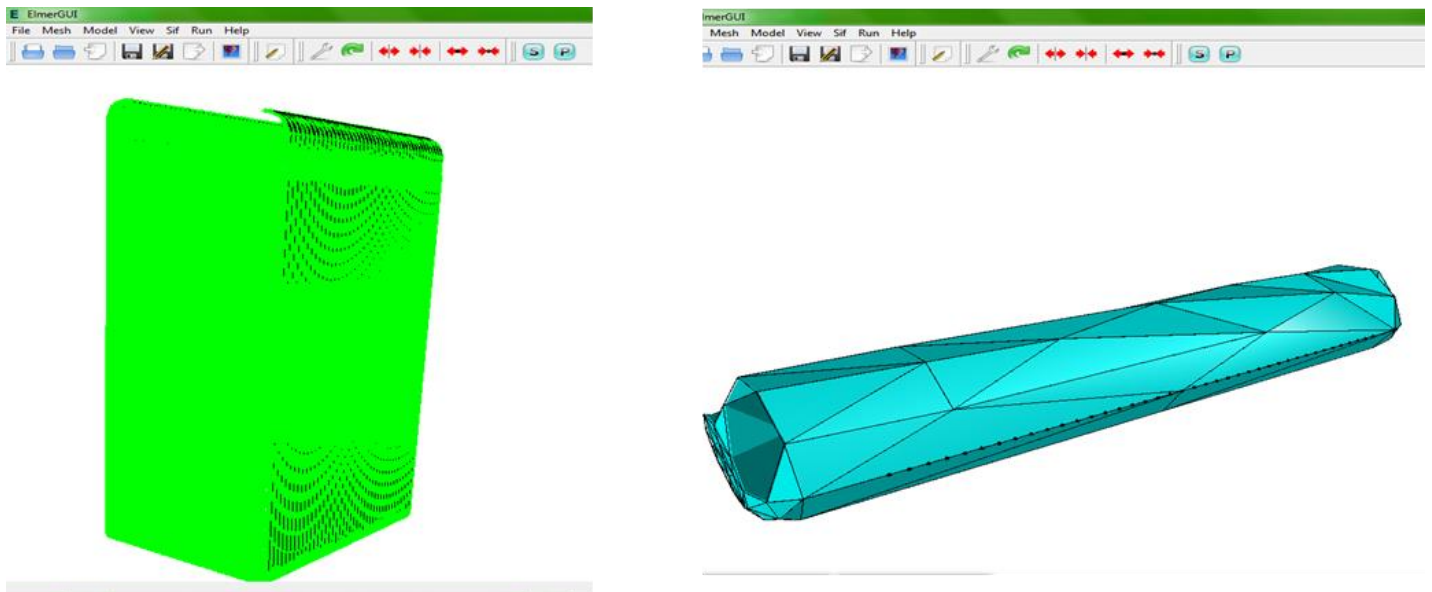


Figure 29: Imported meshed Vaporizer and steam drum in Elmer

The import of the file in .msh format requires a bit of time. Then the initial conditions, the boundary conditions and the type of material for the whole model must be determined. This is a process which about 6 hours.

After putting meshes on the chamber of combustion (evaporator, furnace) and on the drum we have to import this meshes separately to Elmer.

As shown in the figure 2.4.5 we have succeeded to import the mesh of the boiler and also we have determinate the type of material used in this study, the boundary condition and the equation used to determinate the stress.

3.2 Running the solver

After the execution of the work, the Elmer software requires approximately 4 hours to complete the calculations. A "convergence history" window appears on the user interface.

After running the Elmer solver which took a lot of time to finish calculation (approximately 4 hours) without counting the time used to determinate the boundary condition for each body (in the case of boiler we have 40000 body) each one needed to determinate her equation, her material type and his boundary condition (approximately 6 hours). A convergence history appeared during solving us shown in the figure 3.3-3.4:

3.3 Viewing results Paraview / VTK

The unit of the displacement in the figure is meter (m).

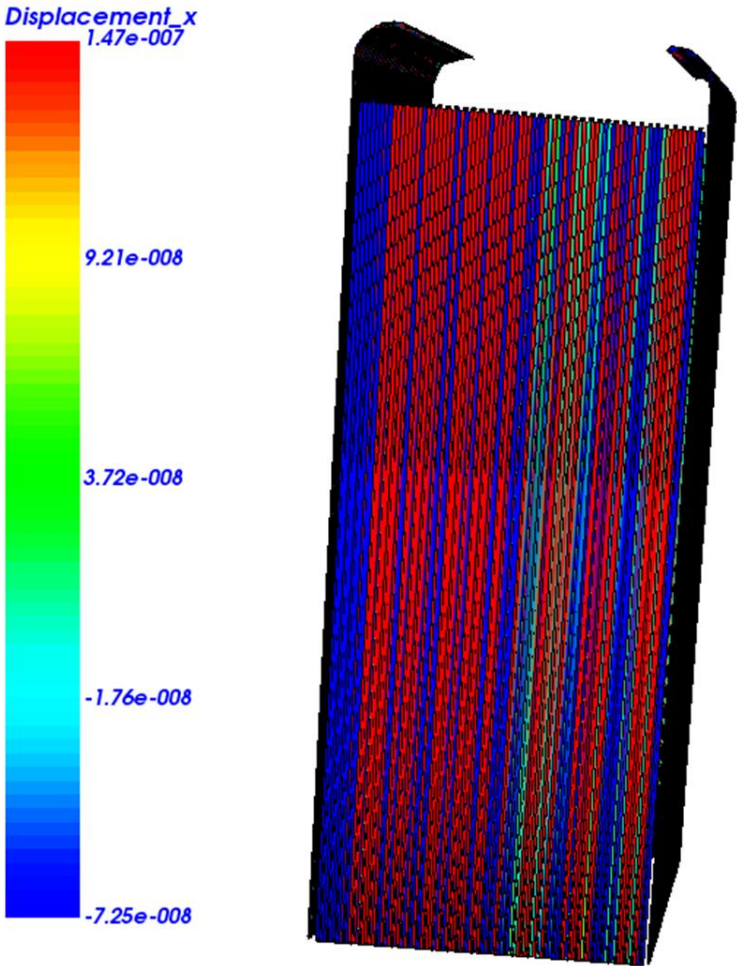


Figure 30: DISPLACEMENT IN THE X DEIRECTION

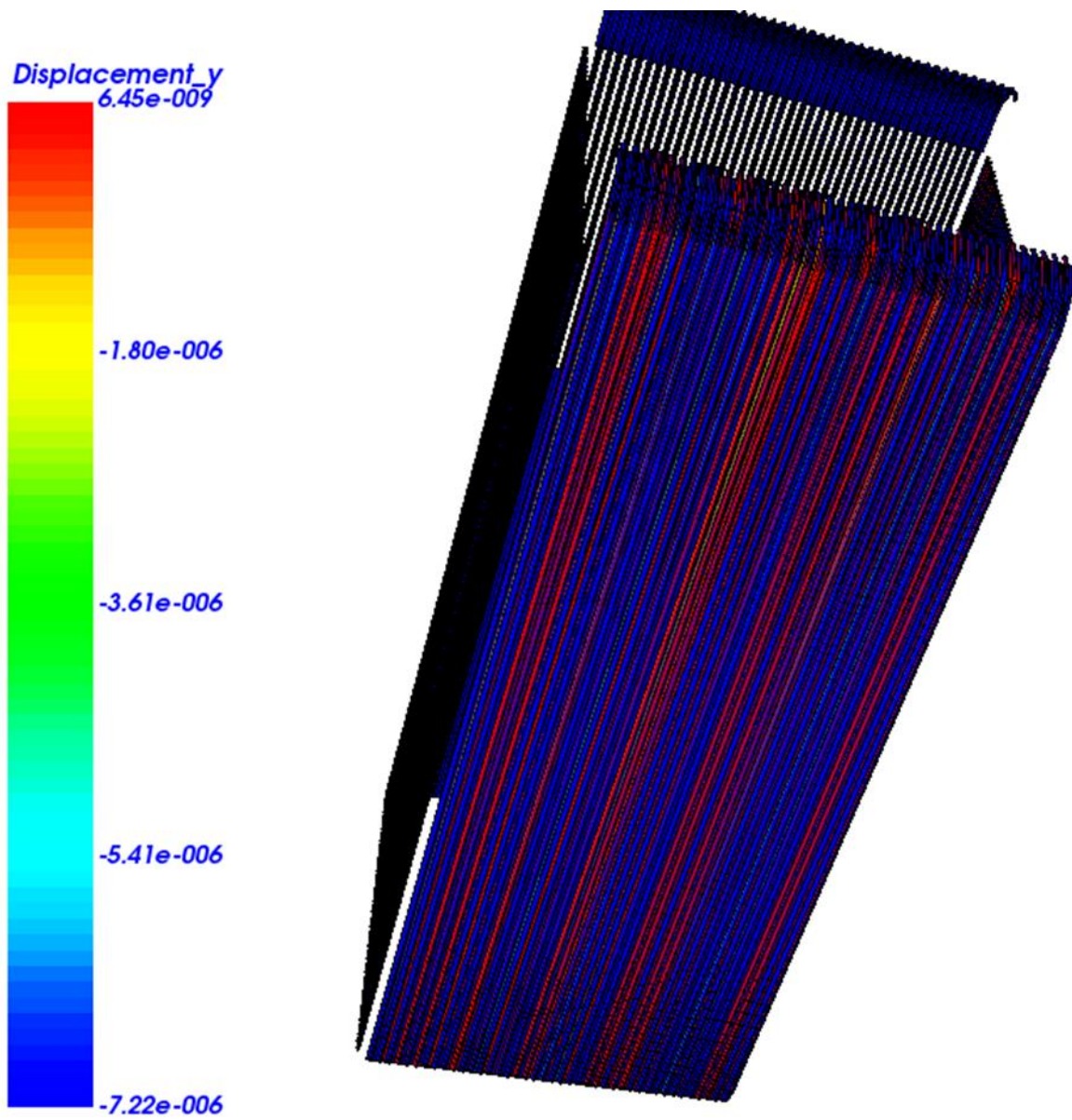


Figure 31: DISPLACEMENT IN THE Y DIRECTION

The unit of the displacement in the figure is meter (m).

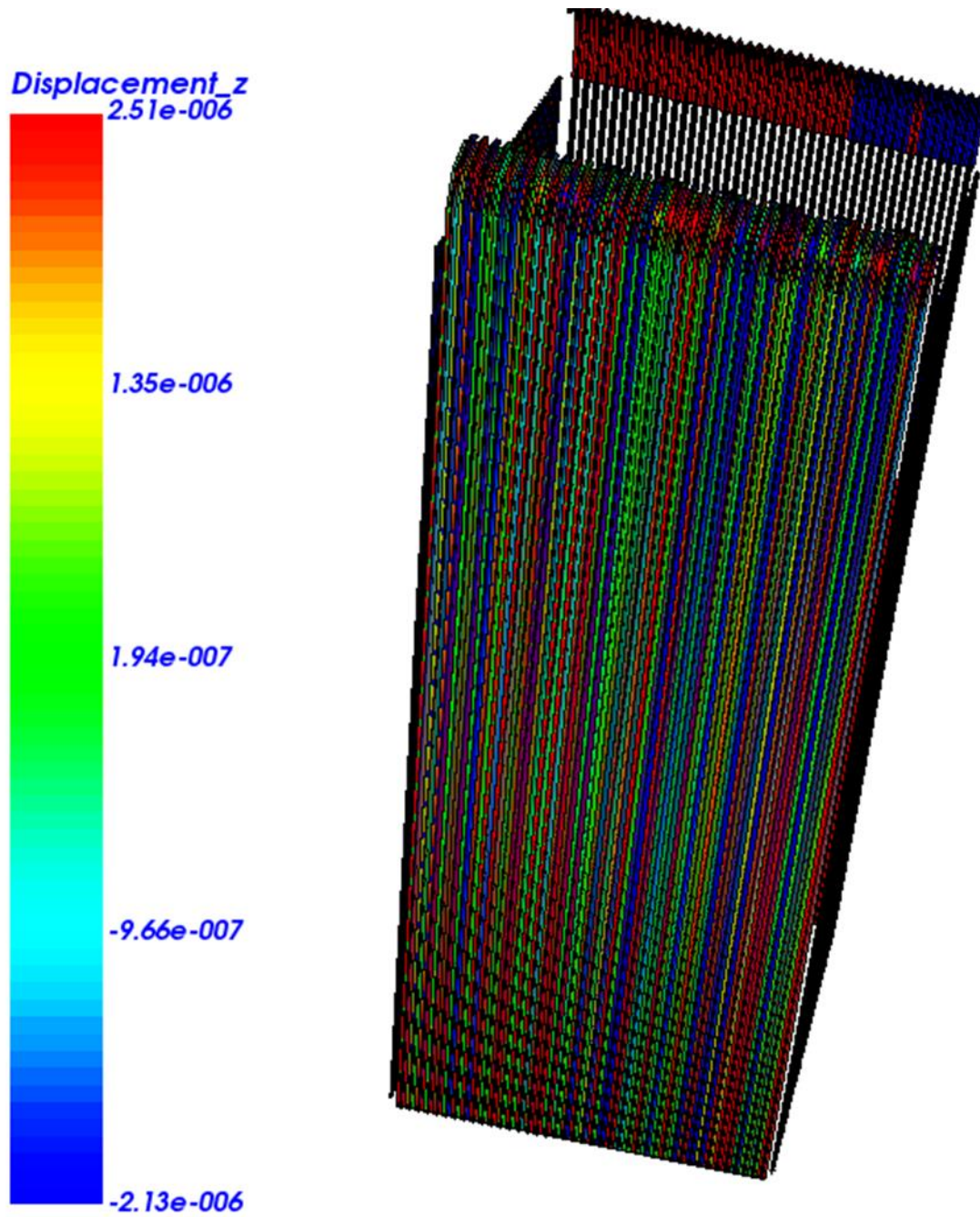


Figure 32: DISPLACEMENT IN THE Z DIRECTION

The unit of the displacement in the figure is meter (m).

In the figure: The unit of the stress is the Pascal (Pa). 1 Pa = 1 N/m²

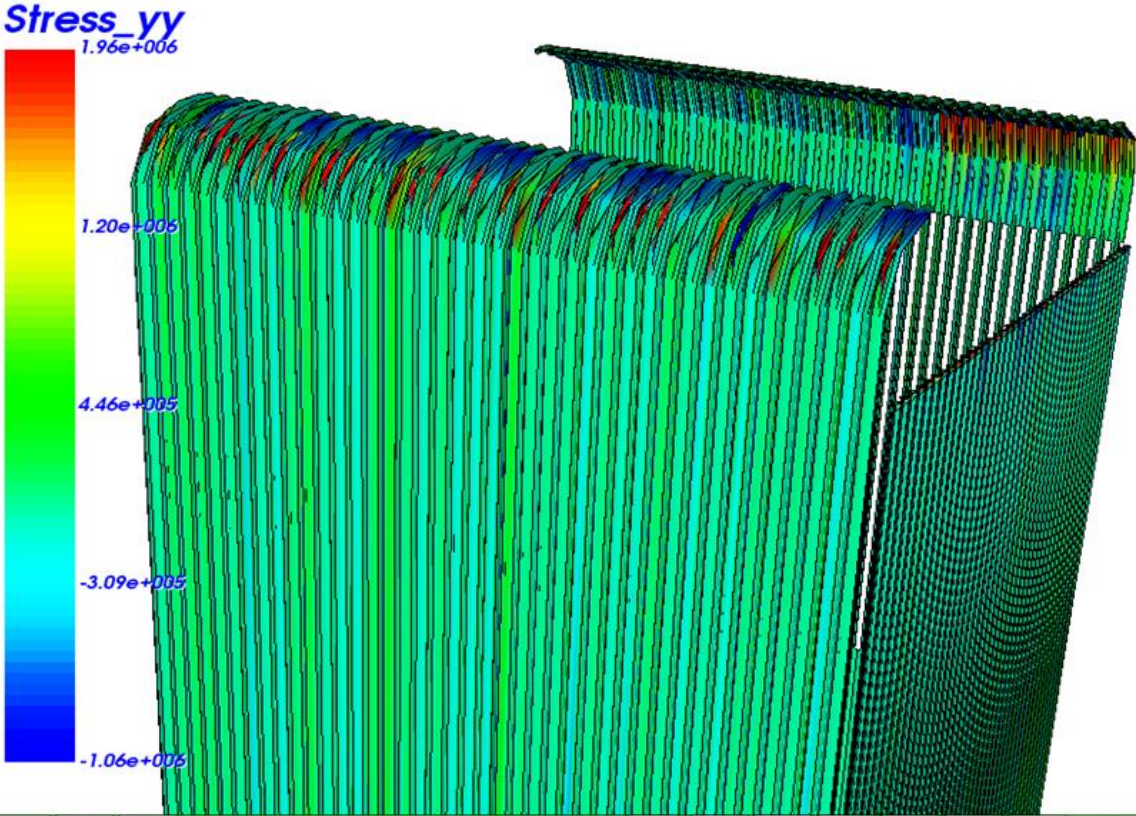


Figure 33: STRESS YY

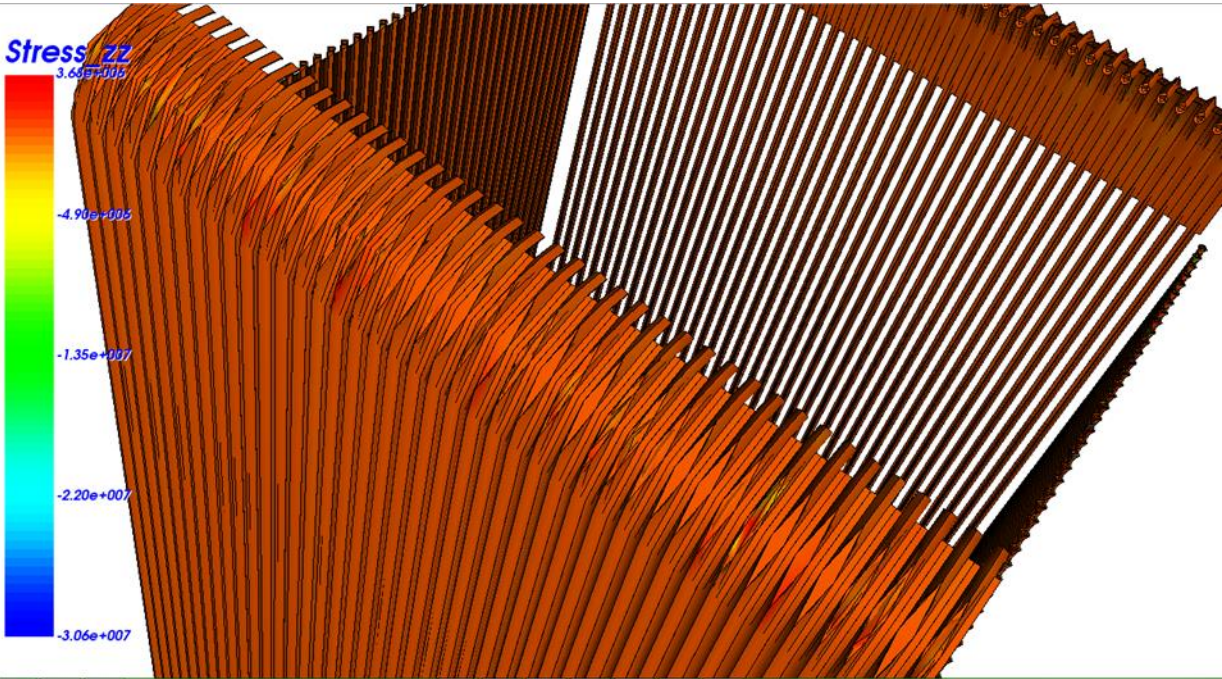


Figure 34: STRESS ZZ

In the figure: The unit of the stress is the Pascal (Pa). 1 Pa = 1 N/m²

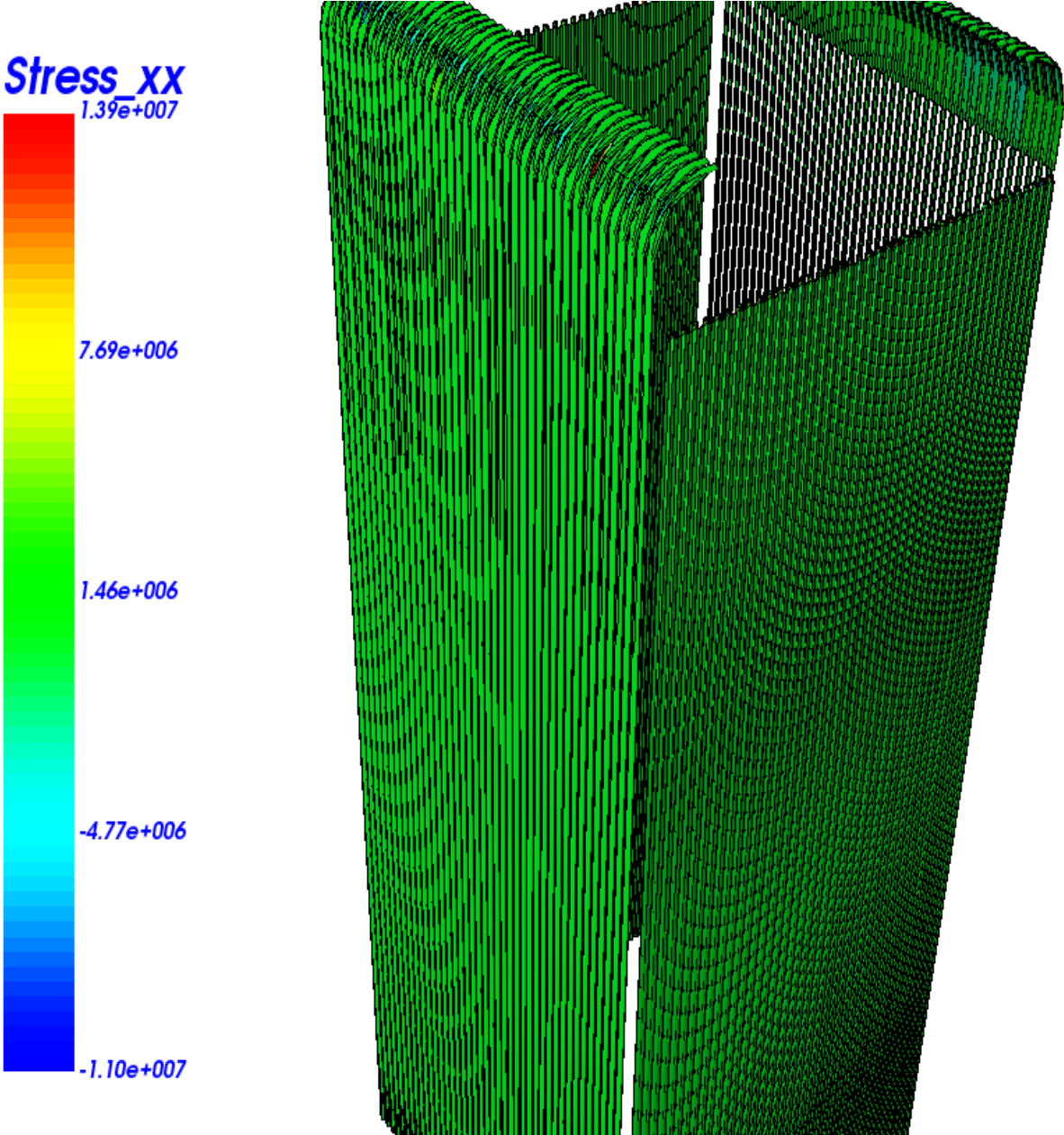


Figure 35: STRESS XX

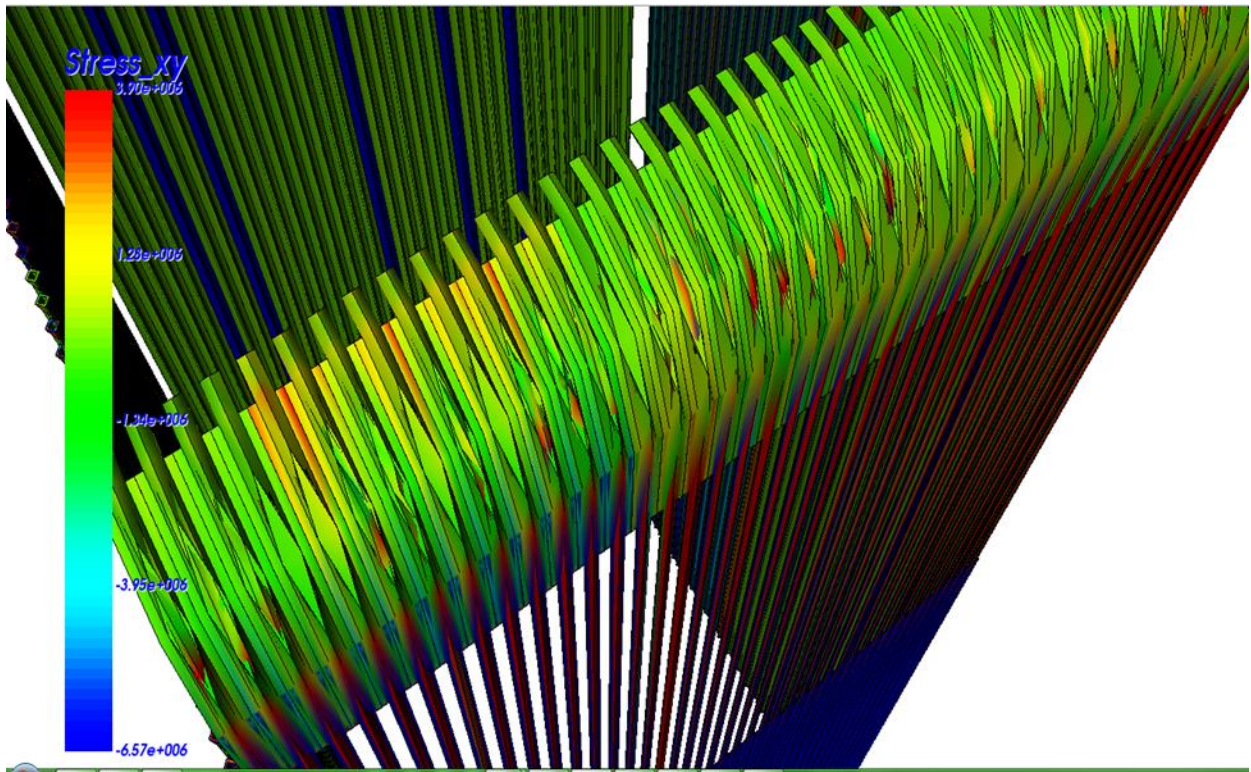


Figure 36: STRESS XY

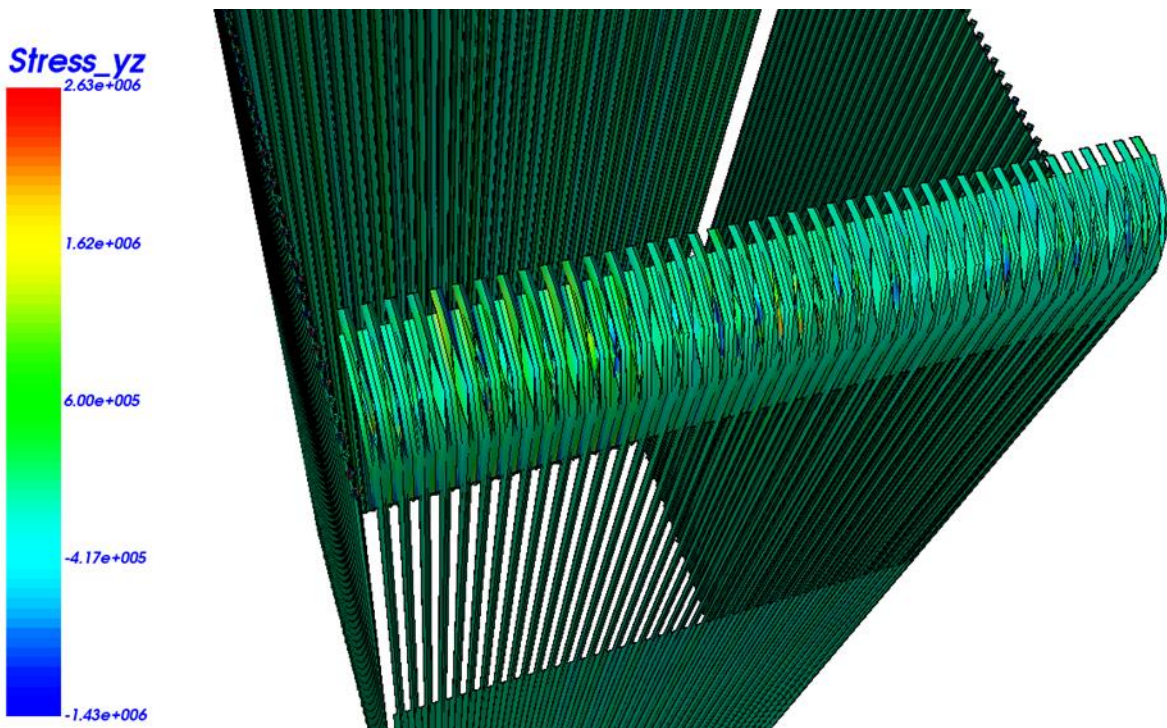


Figure 37: STRESS YZ

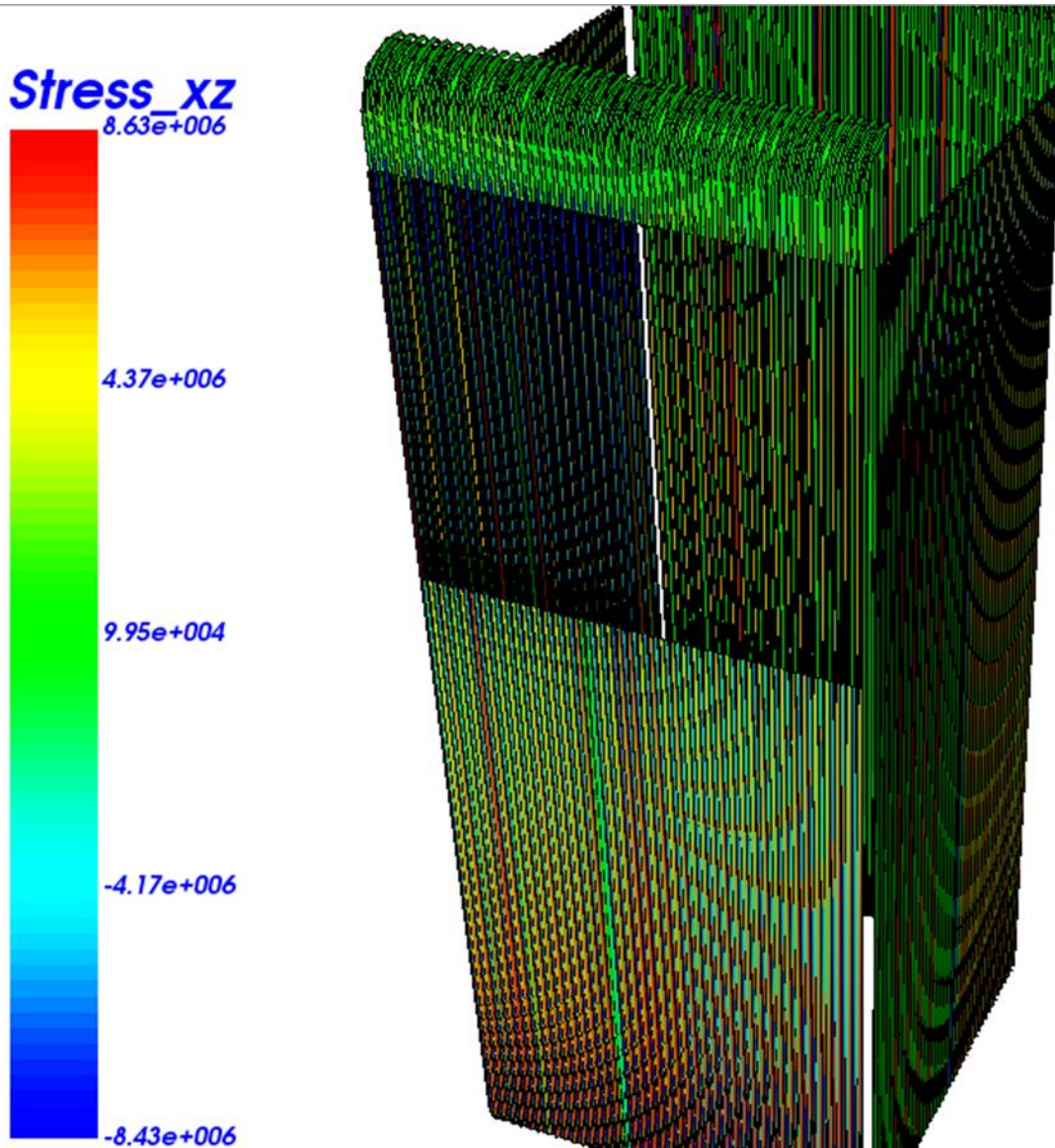


Figure 38: STRESS XZ

In the figure: The unit of the stress is the Pascal (Pa). $1 \text{ Pa} = 1 \text{ N/m}^2$

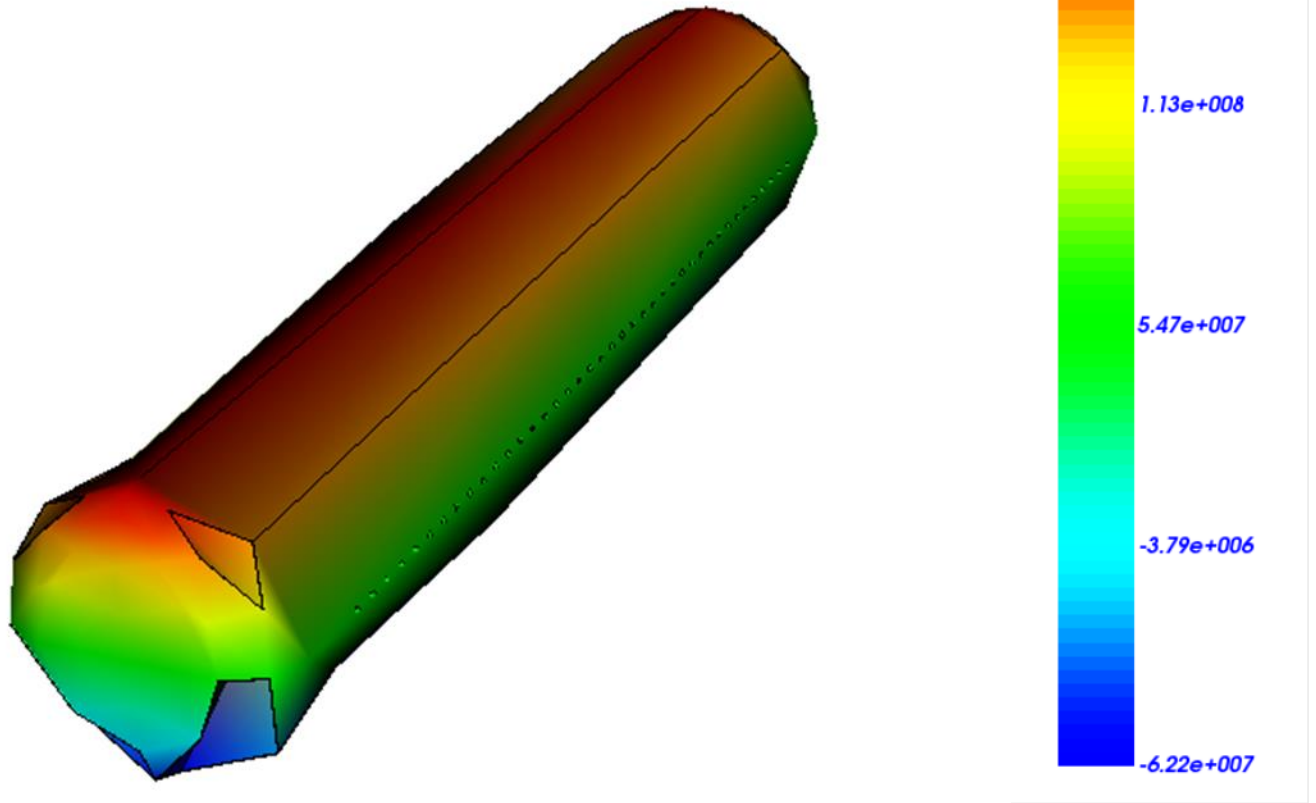


Figure 39: STRESS XX IN THE DRUM

In the figure: The unit of the stress is the Pascal (Pa). $1 \text{ Pa} = 1 \text{ N/m}^2$

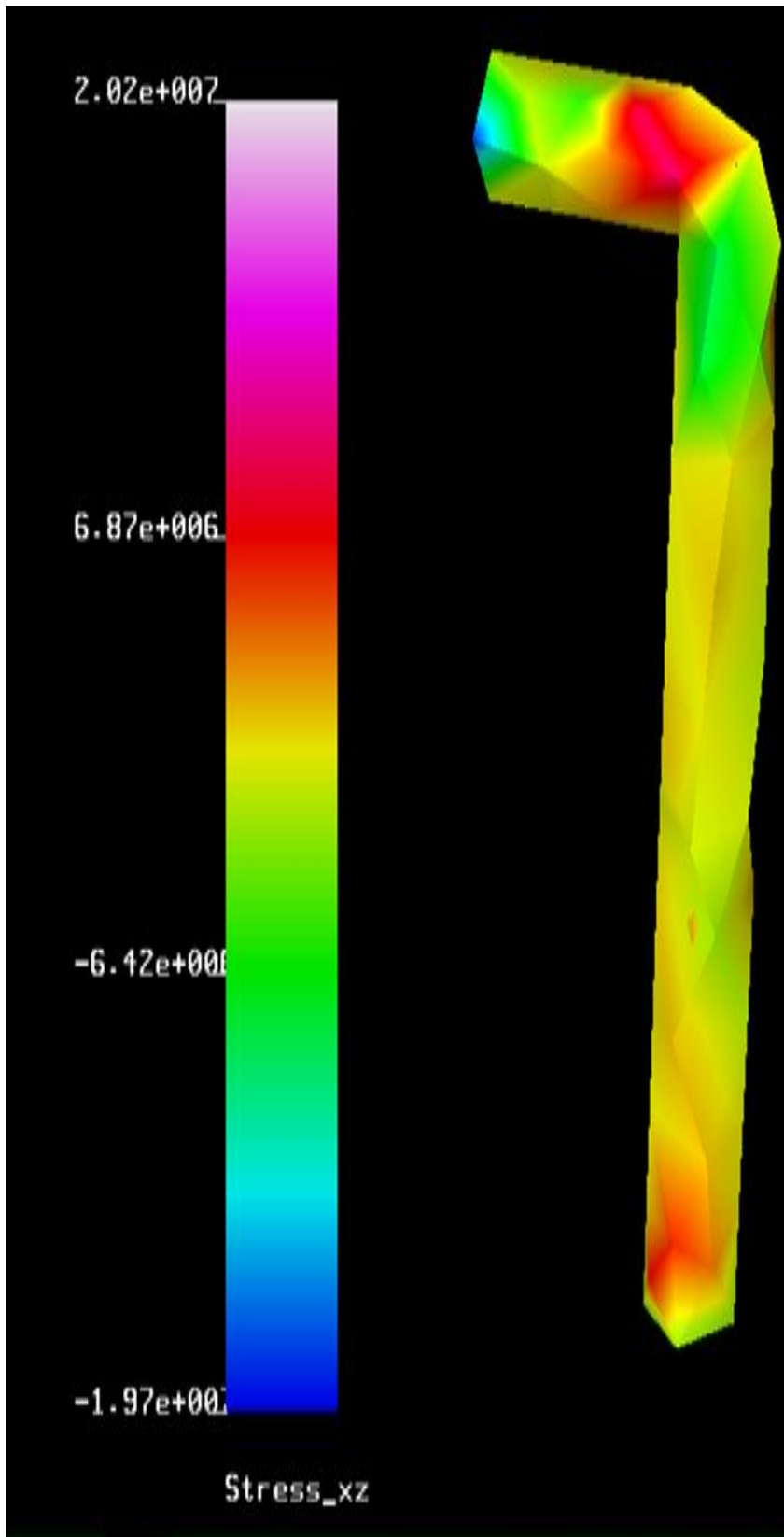


Figure 40: STRESS XZ IN THE TUBE

In the figure: The unit of the stress is the Pascal (Pa). $1 \text{ Pa} = 1 \text{ N/m}^2$

3.4. Estimated number of constant amplitude fatigue cycles

The maximum value considered of 13 MPa is used for calculation of the life due to fatigue at a constant amplitude.

<p>MECHANICAL CONSTANT OF THE STAINLESS STEEL 304L S_{max} or e_{max} = 12 MPa S_{min} or e_{min} = 0 MPa S_a or e_a = 6 MPa S_m or e_m = 6 MPa Material Type = stainless steel Material Name = Stainless Steel 30304, S_u=650.0 S_u = 650 MPa E = 183000 MPa S_{FL} = 147 MPa N_{FL} = 10E+07 $S_{f'}$ = 924 MPa b = -0.114</p>	<p>Surface Finish Type = hot rolled Loading Factor Type = axial k_{size} = 0.1 d = 10 mm K_t = 3.65 Use Fatigue Notch Factor = No K_f = 1 r = 5 mm n = 3 Mean Stress Definition = Maximum Stress Mean Stress Parameter = 13 MPa S_{FL} = 113 MPa k_{SF} = 0.551 k_L = 0.923</p>	<p>RESULTS OBTAINED S_{max} = 13 MPa S_{min} = 12 MPa S_a = 0 MPa S_m = 13 MPa</p>
---	---	--

Table 4: MECHANICAL CONSTANT OF THE STAINLESS STEEL 304L

The estimated number of cycles $N_f = 136000$

3.5. Estimated fatigue safety factor caused by a multiaxial load

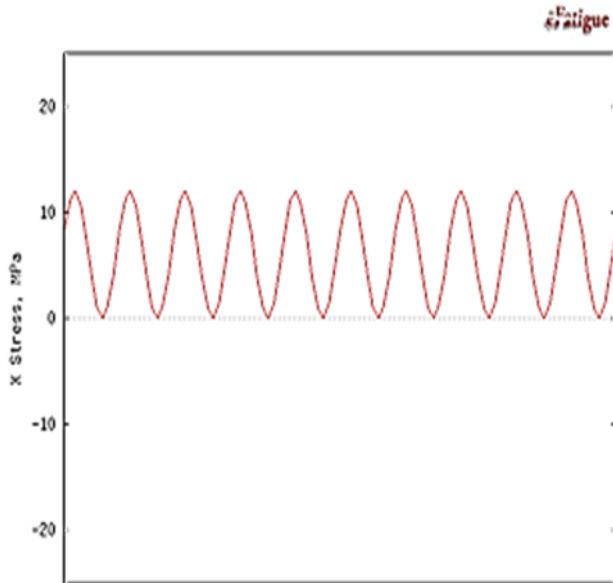


Figure 42: THE STRES IN THE X DIRECTION IN FUNCTION OF THE TIME

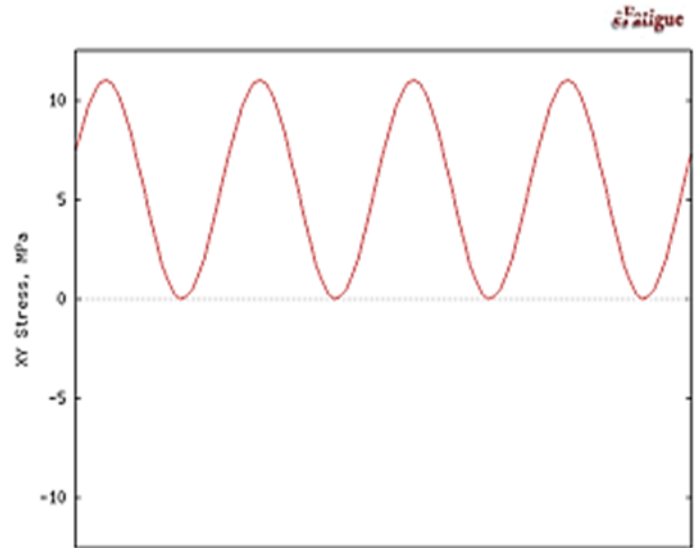


Figure 41: THE STRES IN THE XYDIRECTION IN FUNCTION OF THE TIME

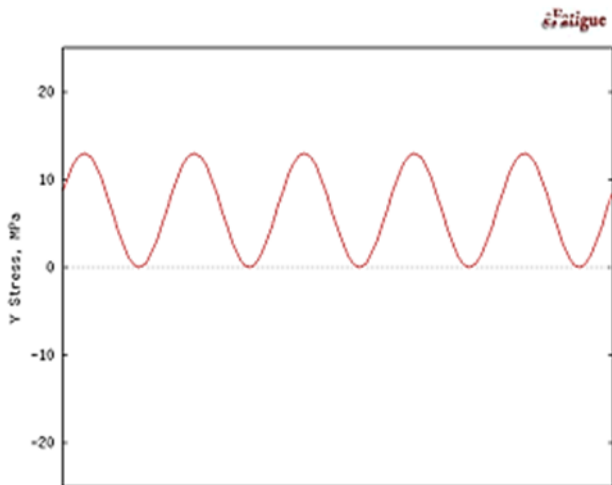


Figure 43: THE STRES IN THE Y DIRECTION IN FUNCTION OF THE TIME

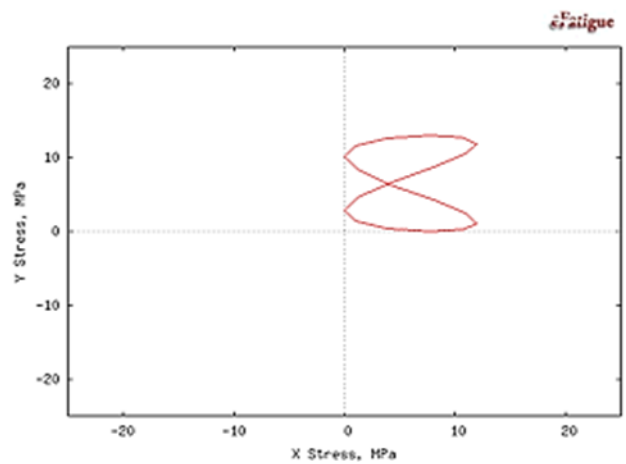


Figure 44: THE STRES IN THE XYDIRECTION IN FUNCTION OF THE STRESS IN THE X DIRECTION

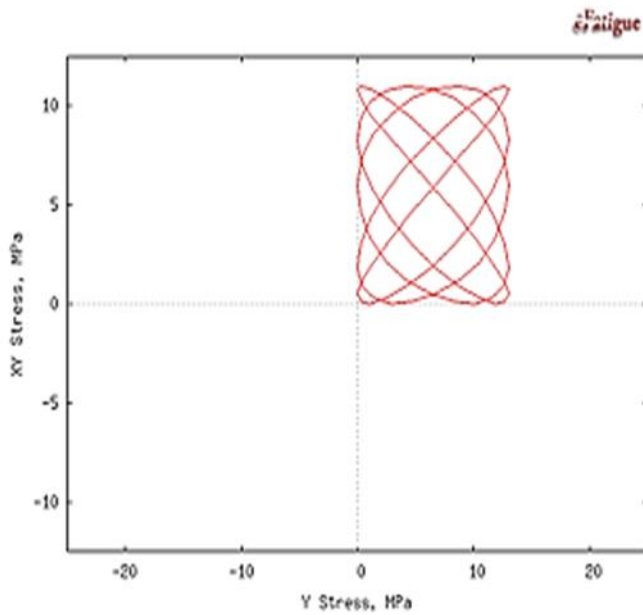


Figure 46: THE STRES IN THE XYDIRECTION IN FUNCTION OF THE STRESS IN THE Y DIRECTION

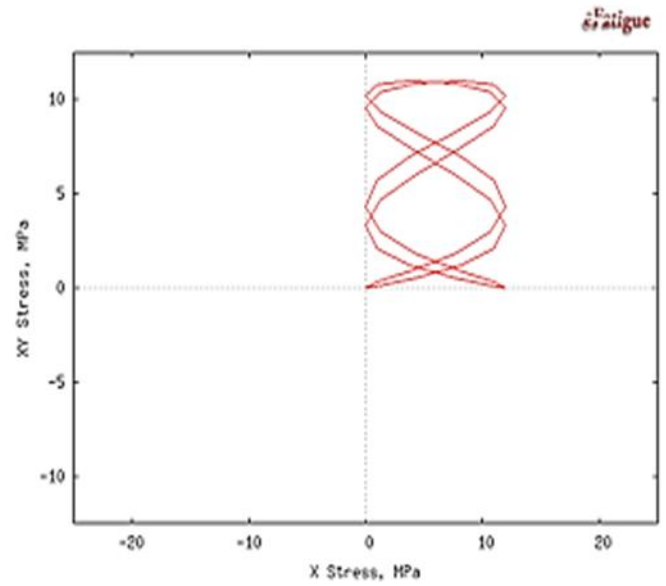


Figure 45: THE STRES IN THE XY DIRECTION IN FUNCTION OF THE STRESS IN THE X DIRECTION

MECHANICAL CONSTANT OF THE STAINLESS STEEL 304L	RESULTS OBTAINED
SFL = 113 MPa	n (Goodman) = 5.768
TFLmax = 73 MPa	n (Findley) = 3.076
Tf'max = 595 MPa	n (Sines) = 3.505
bTmax = -0.114	n (Dang Van) = 4.301e+00
TFLoct = 53 MPa	n (MCE) = 2.958
Tf'oct = 436 MPa	
bToct = -0.114	
G = 73200 MPa	
kFindley = 0.300	
αSines = 0.150	
aDV = 0.400	
bDV = 73 MPa	

Table 5: CALCULATION OF THE SAFETY FACTOR

3.6. Probabilistic analysis of the number of fatigue cycles.

		Deterministic	Probabilistic		
Variable	Value	Sensitivity	Sensitivity	Mean	COV
Loading			0		
S_{\max} or e_{\max}	13 MPa	-2.41	0.00	13	0.000
S_{\min} or e_{\min}	0 MPa	0.00	0.00	0.00e+00	0.00e+00
Material Properties			0.15		
S_u	650 MPa	2.23	0.00	650	0.000
S_f'	L(924 MPa,0.10,0.90)	-0.77	0.15	928	0.099
b	C(-0.114,0.00,1.00)	-3.07	0.00	-0.114	0.047
Surface Finish			0.88		
k_{SF}	N(0.551,0.10)	2.00	0.88	0.550	0.099
Stress Concentrators			0.45		
K_f	N(3.65,0.05)	-2.04	0.45	3.65	0.050

Table 6: Probabilistic analysis of the number of fatigue cycles.

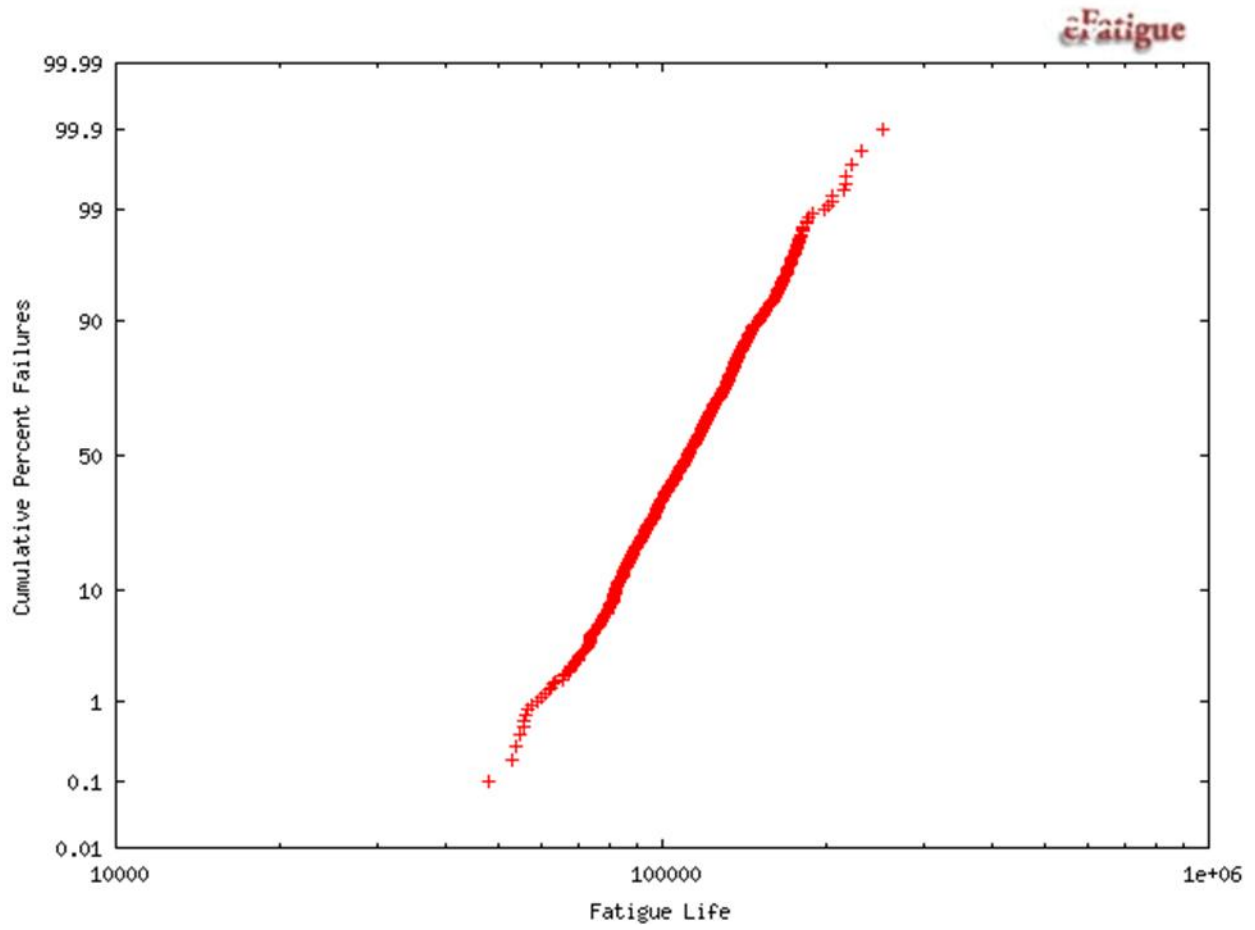


Figure 47: THE CUMULATIVE PERCENT FAILURES IN FUNCTION OF FATIGUE LIFE

Nf , median = 111215 cycles

3.7. Estimate of the number of cycles of elongation at constant amplitude

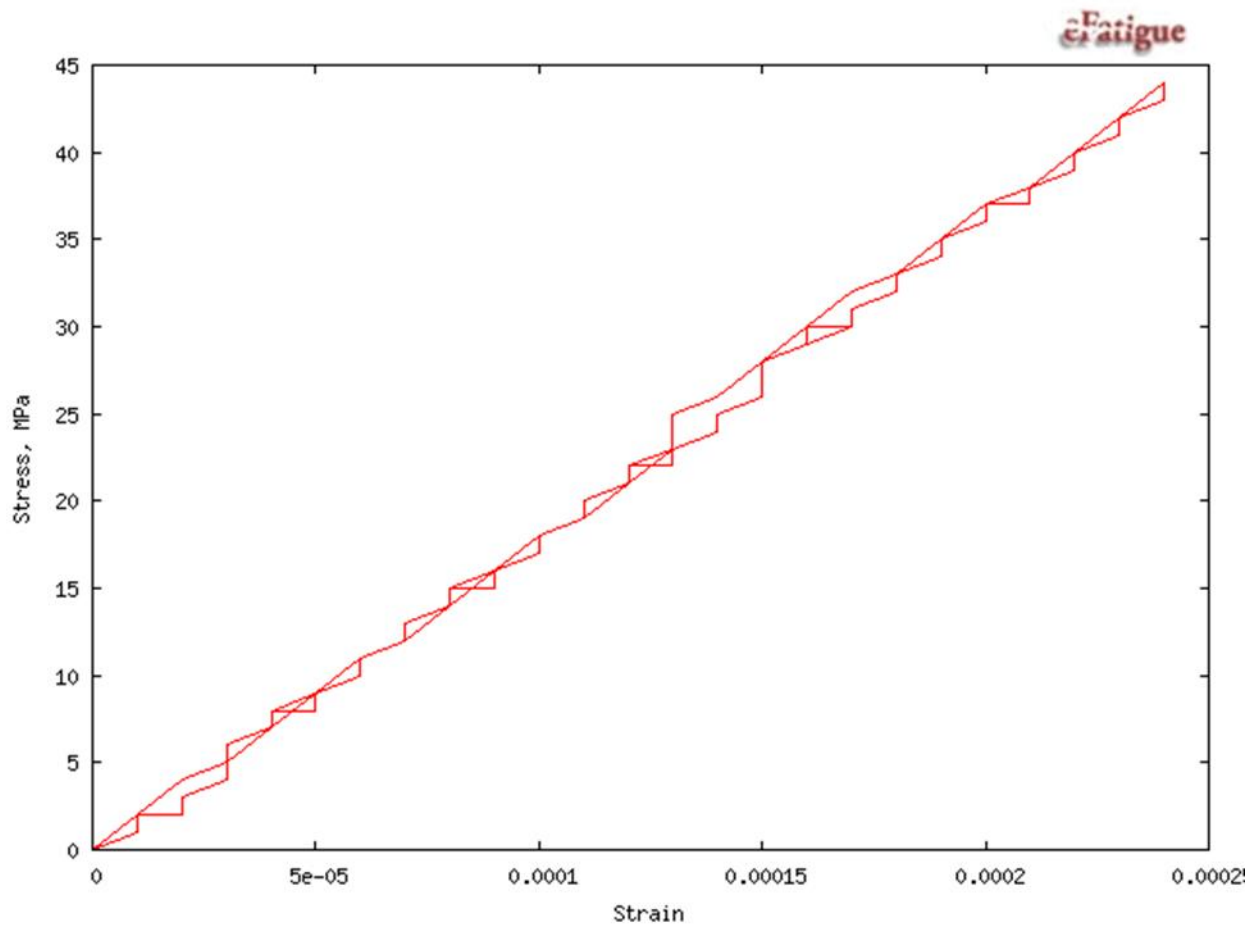


Figure 48: THE HYSTHERESIS LOOP

Nf = > Limite de la fatigue 50000000 cycles , n ~ 6.12

3.8. Estimated number of cycles due to displacement caused by a multiaxial load

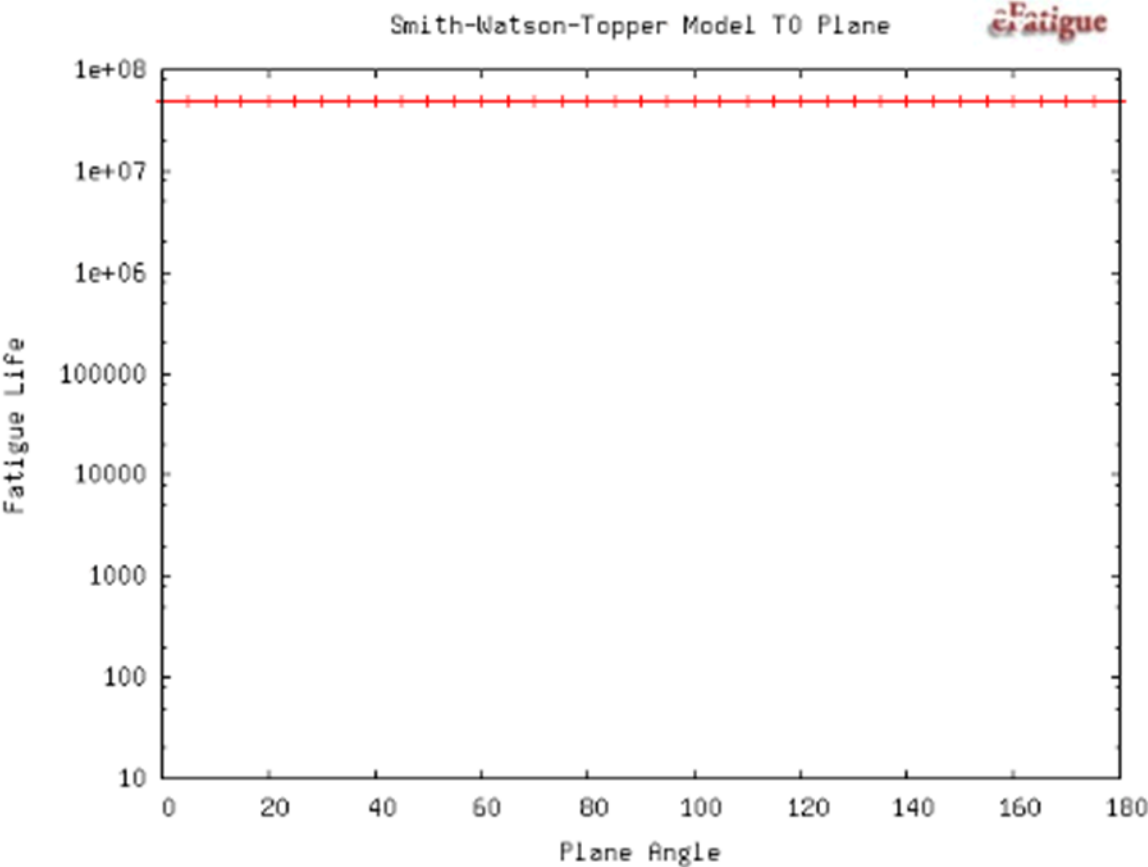


Figure 49: SMITH-WATSON-TOPPER MODEL

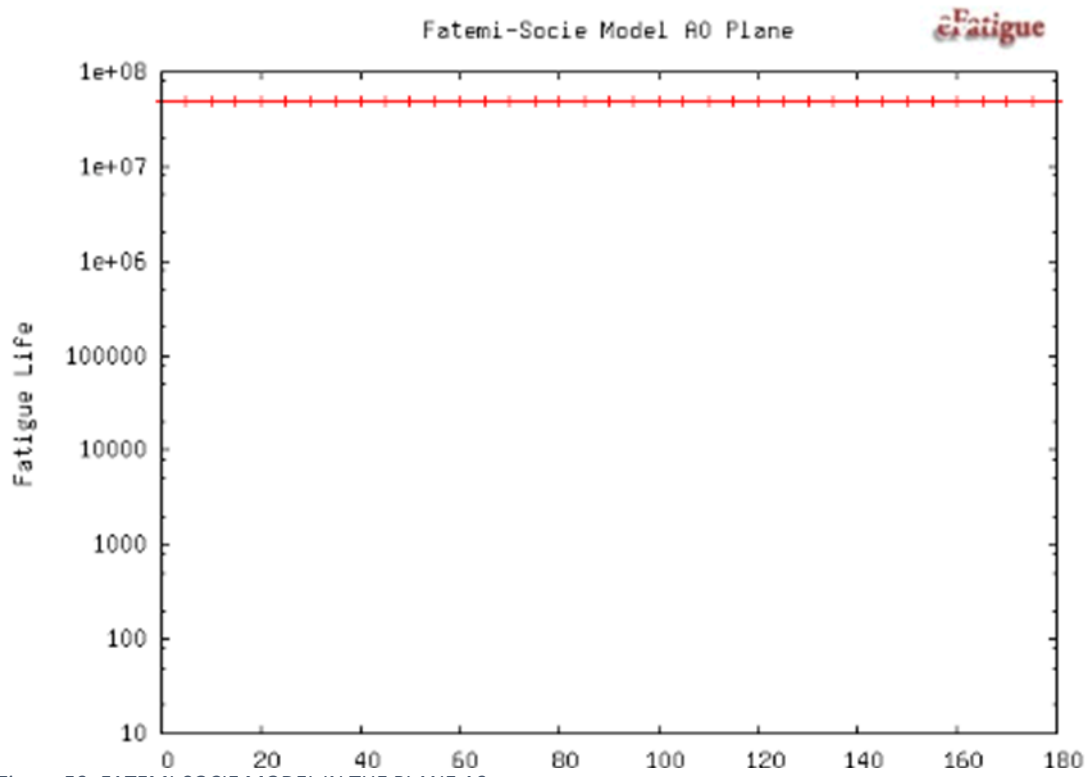


Figure 50: FATEMI-SOCIE MODEL IN THE PLANE A0

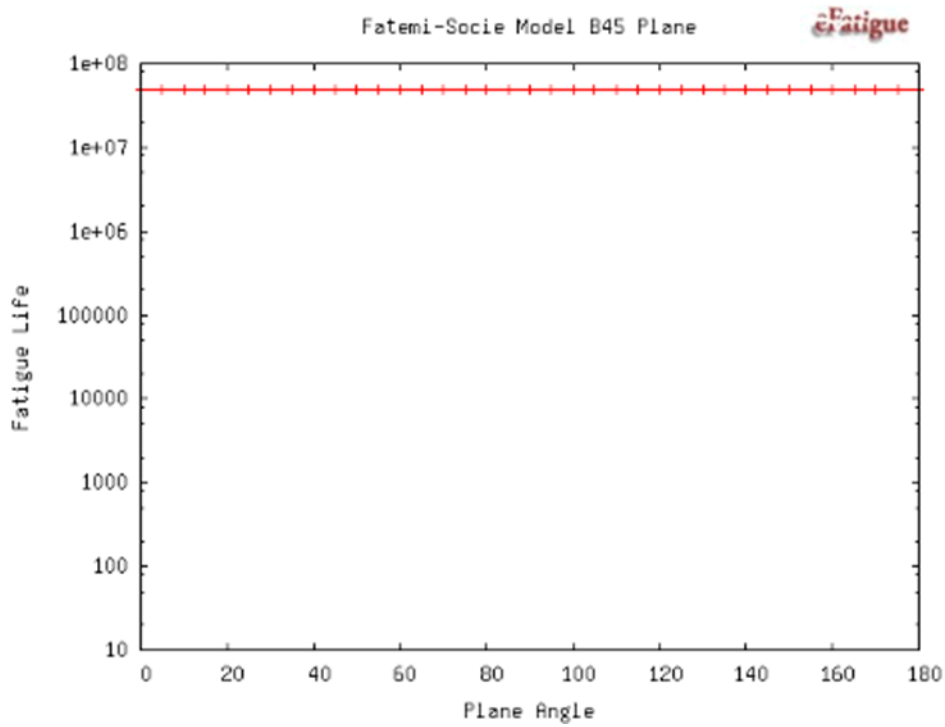


Figure 51: FATEMI-SOCIE MODEL IN THE PLANE B45

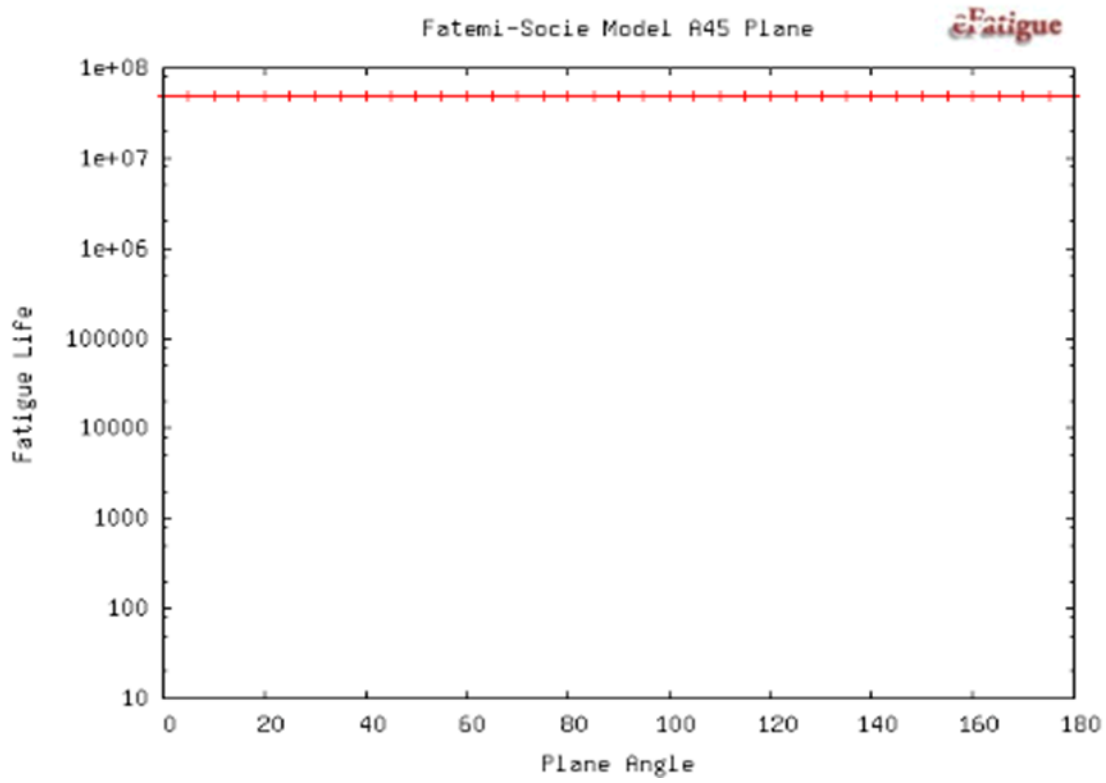
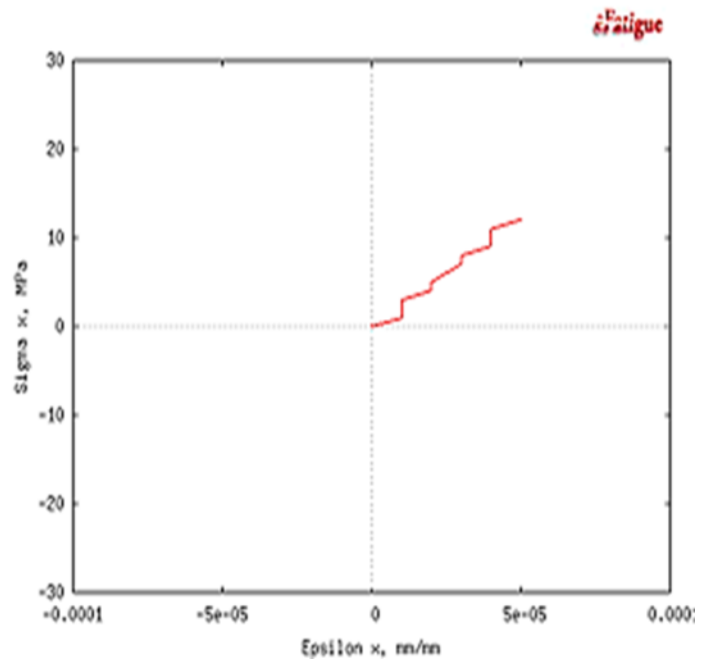
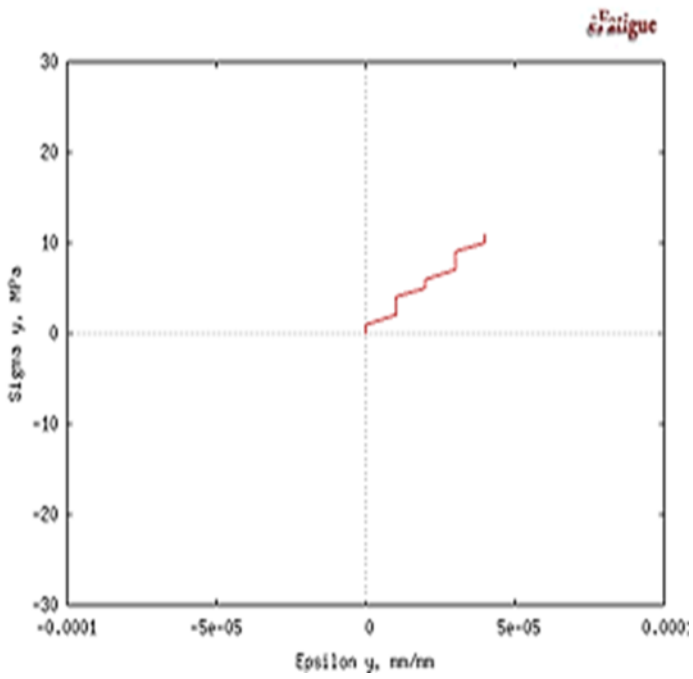
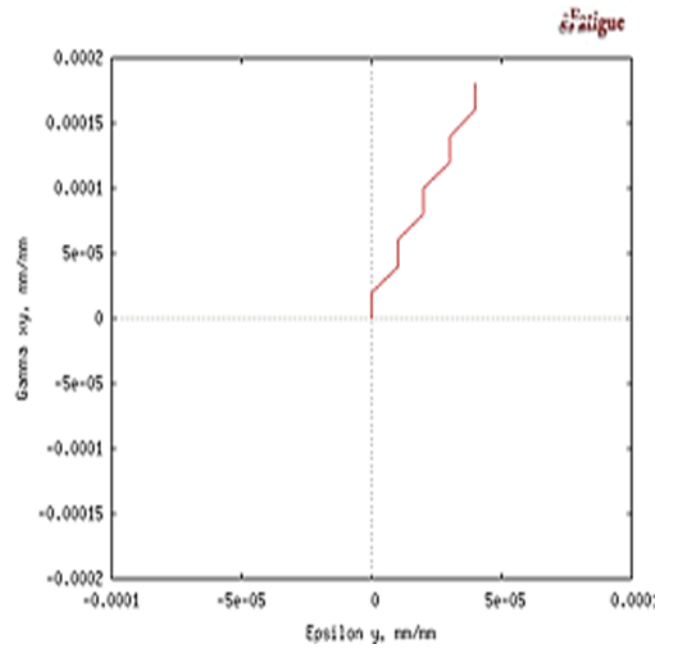
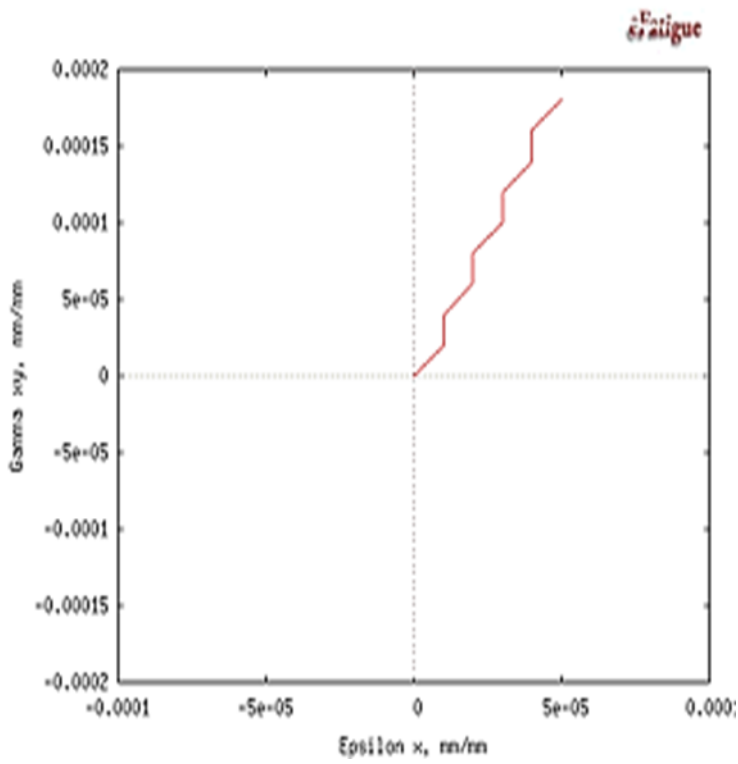
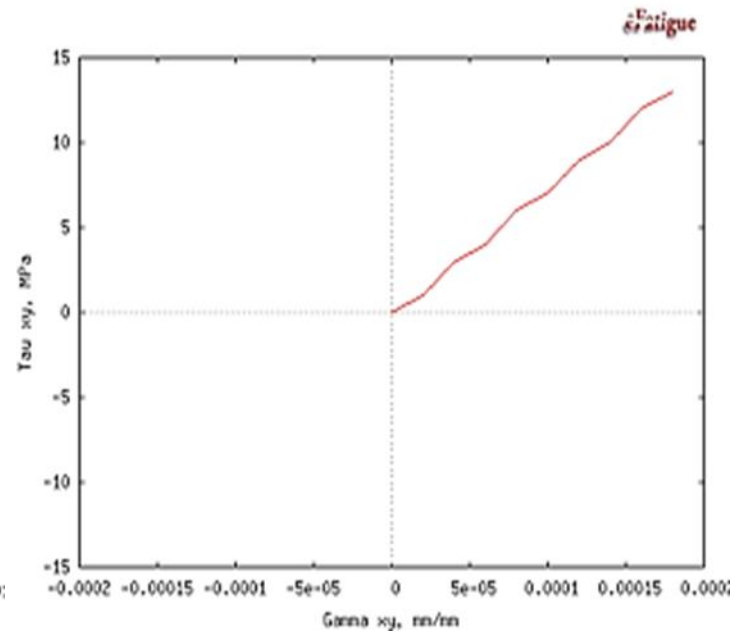
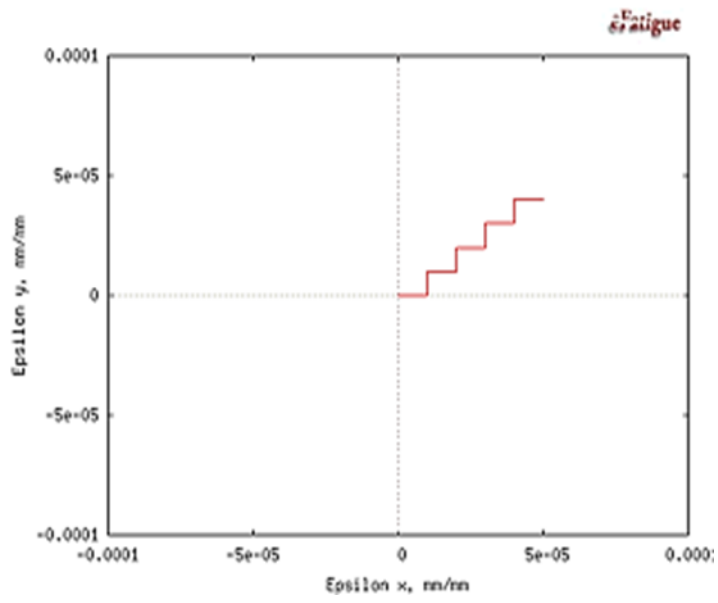


Figure 52: FATEMI-SOCIE MODEL IN THE PLANE A54





3.9. Results of Fallo software

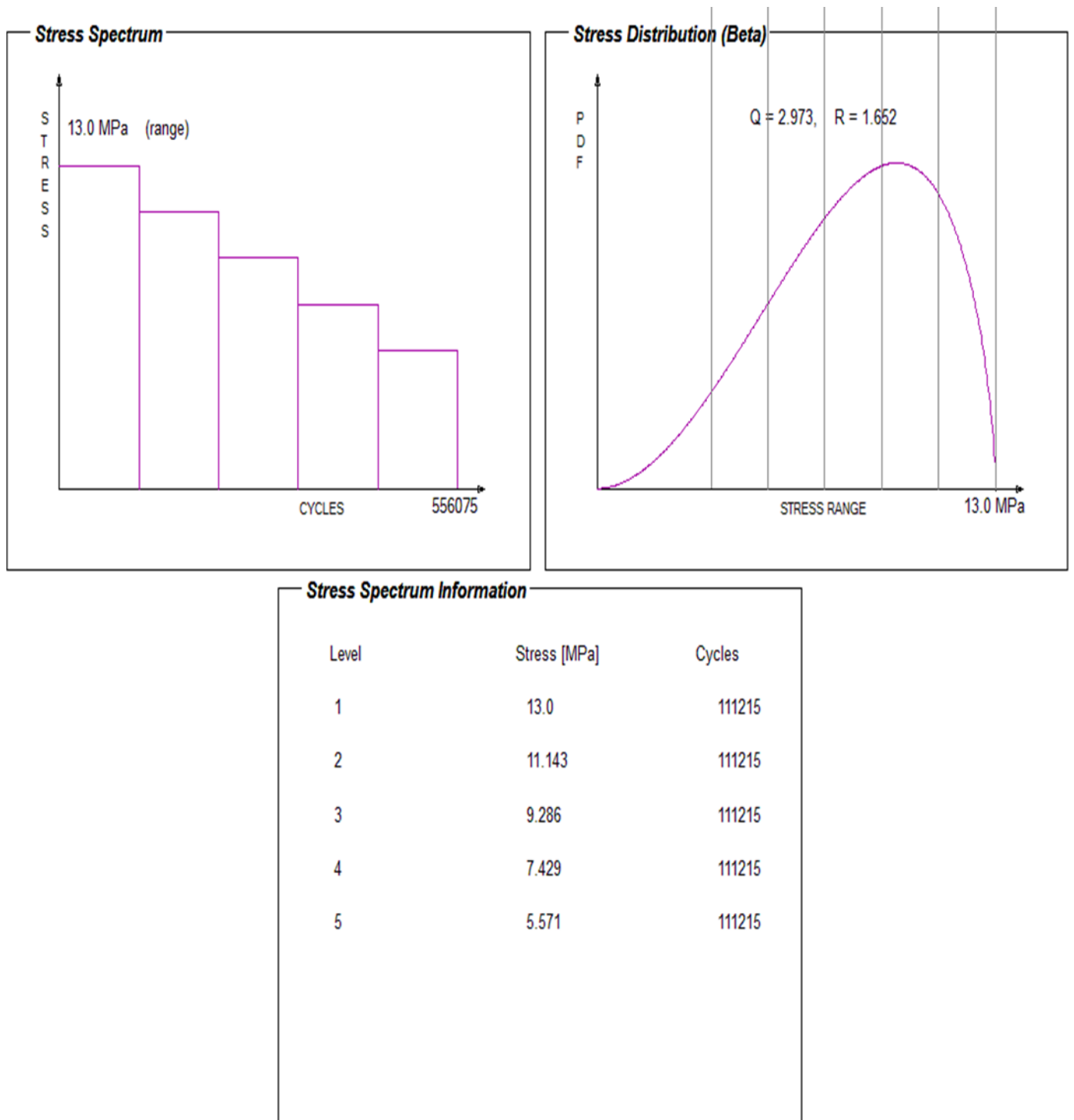


Figure 53: Results of Fallo software

3.10. Results of FALSN software

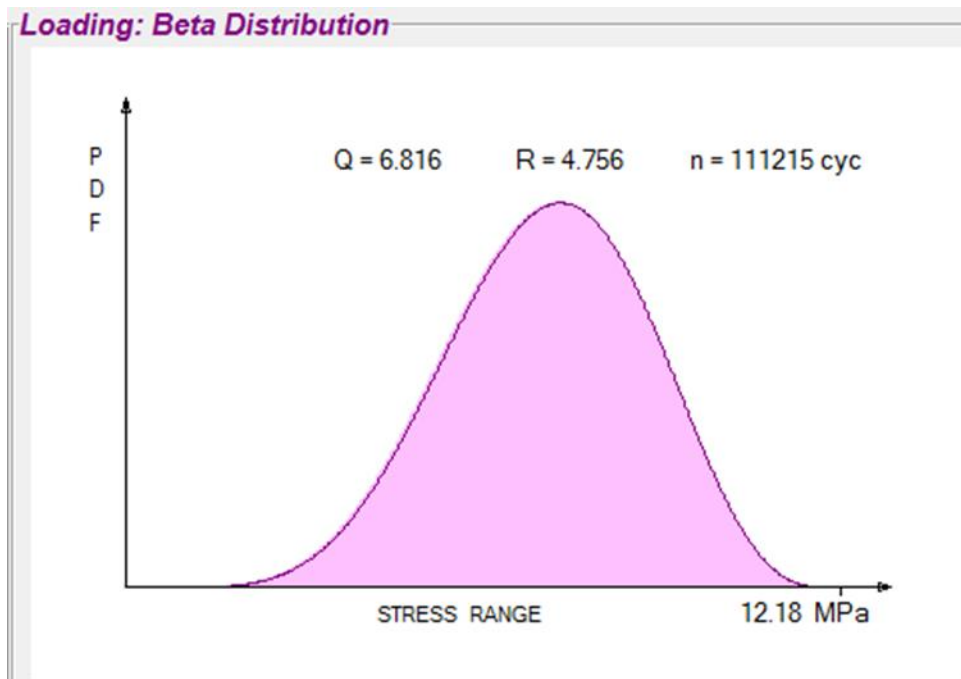


Figure 54. BETA DISTRIBUTION

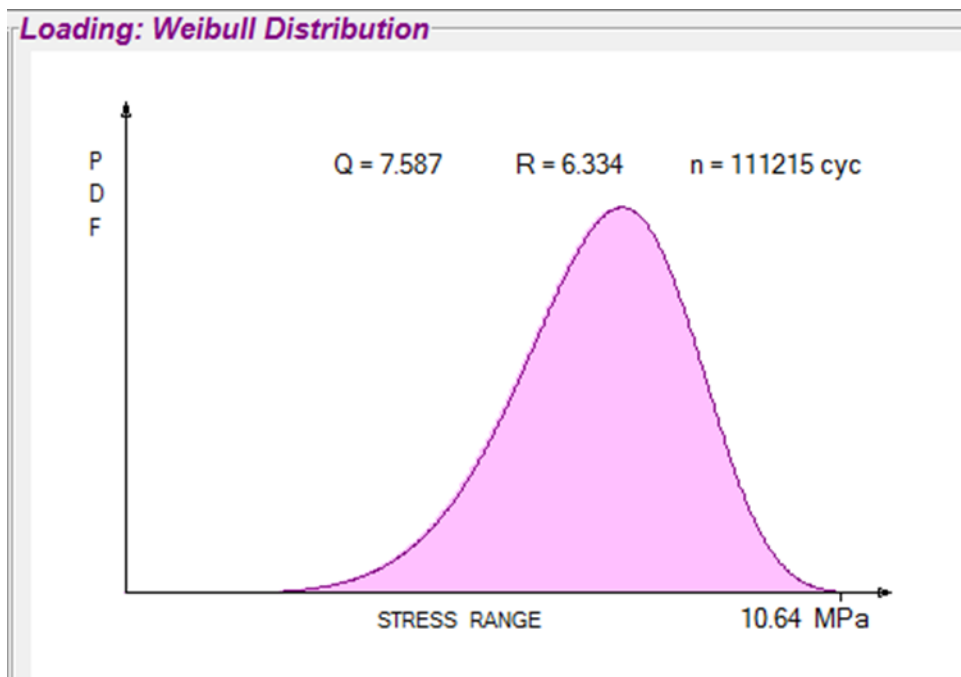


Figure 55: WIEBULL DISTRIBUTION

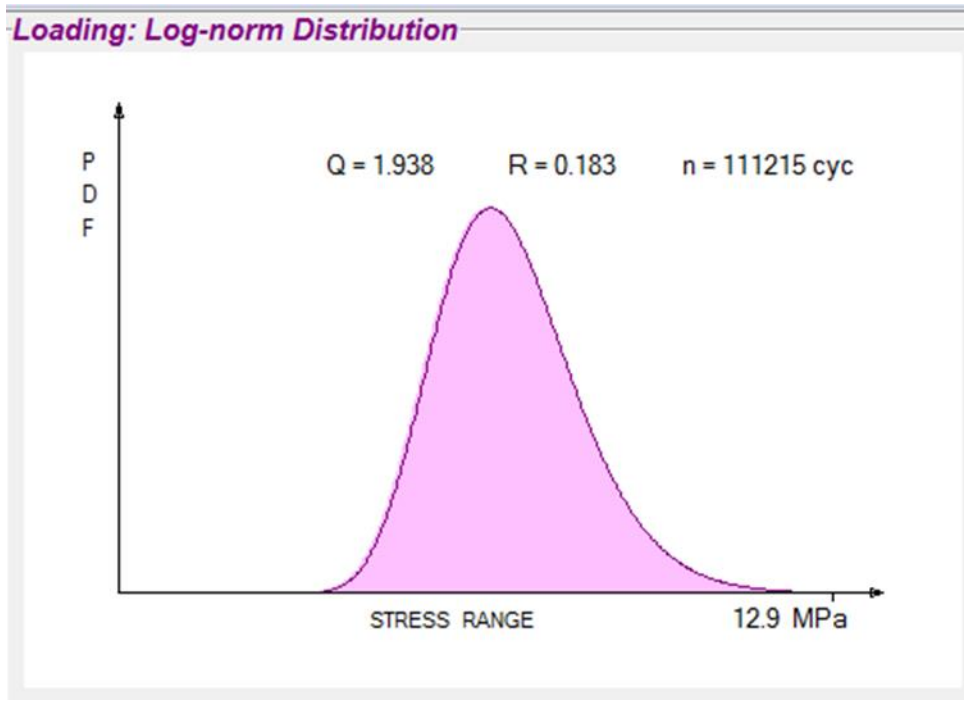


Figure 56: LOD-NORM DISTRIBUTION

3.11. Results of FALIN software

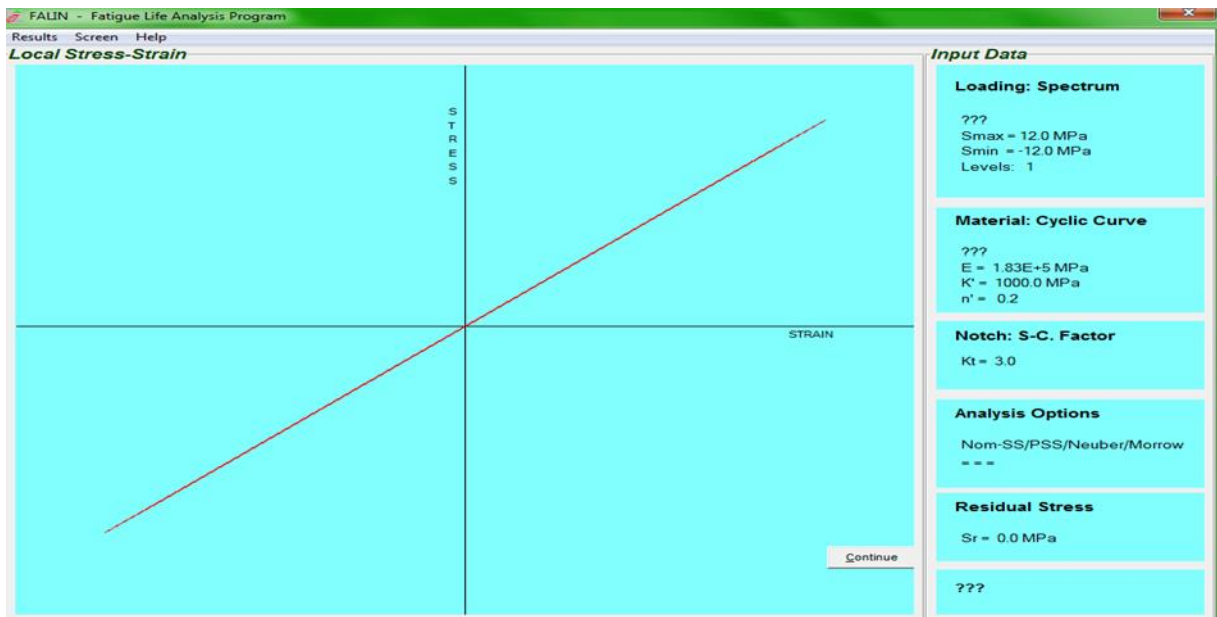


Figure 57: Results of FALIN software

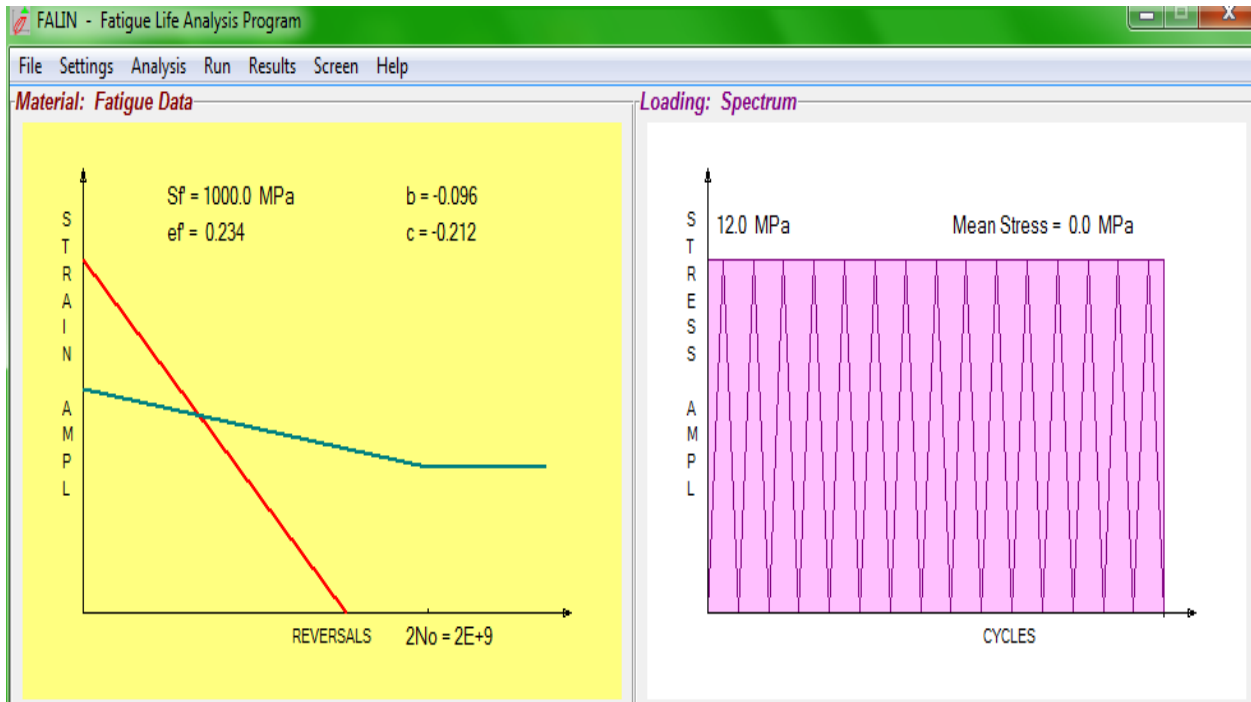


Figure 58: FATIGUE DATA

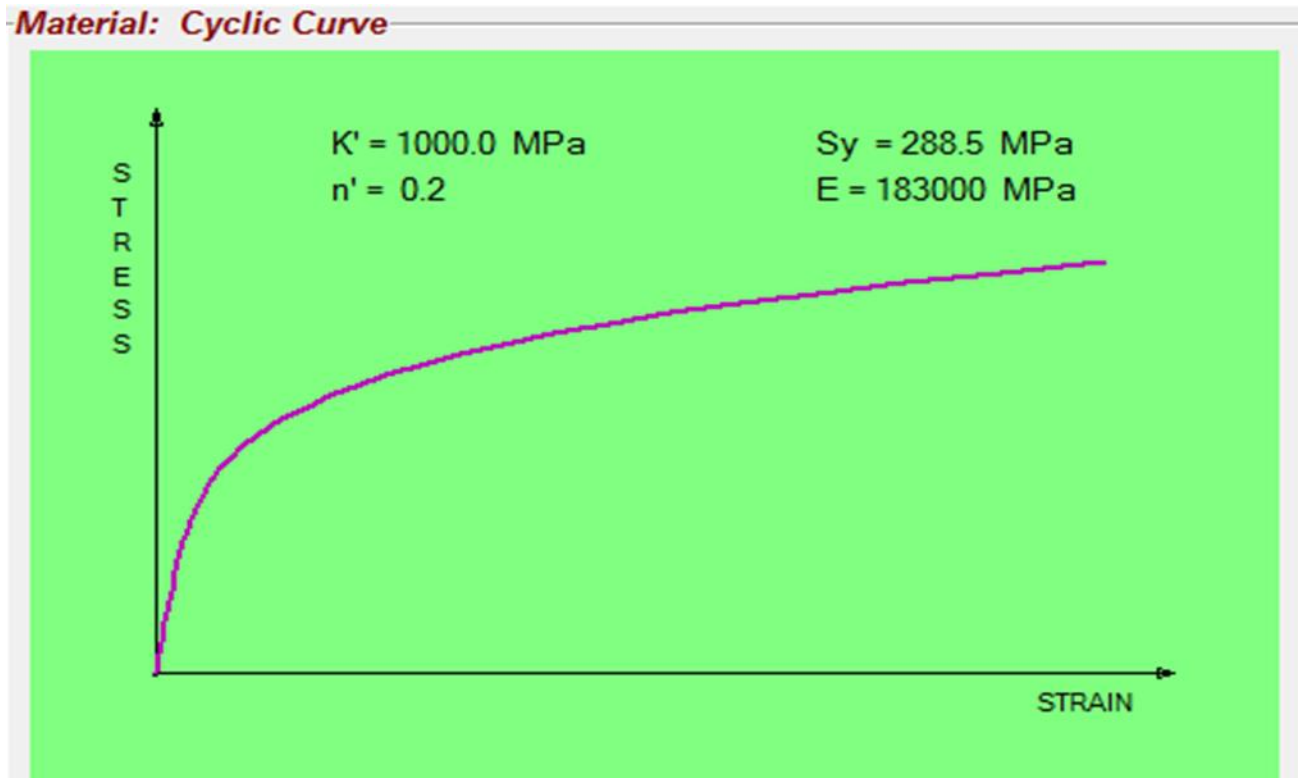


Figure 59: CYCLIC CURVE

3.12. Discussions of all results

In the figure shown above, it is clear that the stress distribution undergoes significant variation during the passage of fluid in the tube neck. This enormous variation is expected and planned, since steam has a significant speed and pressure and it will undergo two flow direction changes during a short time.

Moreover, of the number of cycles calculated in previous sections, the one we chose to lower value to avoid any risk.

The lowest number received is $N = 111215$, followed by the number of cycles multiplied by the time during which it stops the operation of the apparatus, and it was found that the time of operation before the break is almost 20 years .

CHAPTER IV: CONCLUSION AND FUTURE WORK

About the technological side, Elmer simulation requires a long time to determine the initial and boundary conditions, and then it is recommended to make a script to get rid of and to reduce the time.

And finally this study does not take into account or stress due to the high temperature or the effect of corrosion caused by steam. In addition, these two conditions are able to reduce the lifetime of the vaporizer.

BIBLIOGRAPHY

- [0] S. Mourad, TEMO-STPP/IPP, 5th project report, published on www.aecenar.com, AECENAR, , Ras Nhache/Batroun, Lebanon, 2014
- [1] Introduction to fracture mechanics, David Roylance, Massachusetts Institute of technology, Cambridge MA 02159, June 2001, pg.1
- [2] Treatment of Power Industry Wastes Lawrence K. Wang Lenox Institute of Water Technology and Krofta Engineering Corporation, Lenox, Massachusetts and Zorex Corporation, Newtonville, New York, U.S.A., Vol.13,pg. 581
- [3] Pressure Vessels Design and Practice, Somnath Chattopadhyay, CRC Press 2005, pg. 39-45
- [4] Forrest, Fatigue of Metals, Pergamon Press, London, 1962
- [5] Noll and Lipson, "Allowable Working Stresses", Society for Experimental Stress Analysis, Vol. III, no. 2, 1949
- [6] MacGregor and Grossman, "Effects of Cyclic Loading on Mechanical Behavior of 24S-T4 and 75S-T6 Aluminum Alloys and SAE 4130 Steel", NACA TN 2812, 1952
- [7] Gmsh: a three-dimensional finite element mesh generator with built-in pre- and post-processing facilities, INTERNATIONAL JOURNAL FOR NUMERICAL METHODS IN ENGINEERING, Christophe Geuzaine, Jean-François Remacle, 2002
- [8] Elmer Models Manual, Peter Råback, Mika Malinen, Juha Ruokolainen, Antti Pursula, Thomas Zwinger, Eds. CSC – IT Center for Science, April 30, 2015
- [9] Forman, Hickman and Shivakumar "Stress Intensity Factors for Circumferential Through Cracks in Hollow Cylinders Subjected to Combined Tension and Bending Loads" Engineering Fracture Mechanics, Vol. 21, No. 3, 563-571, 1985
- [10] Erdogan and Ratwani "A Circumferential Crack in a Cylindrical Shell under Torsion" International Journal of Fracture, Vol. 8 , No. 1, 87-95, 1972
- [11] Reference Guide Du Dessinateur Les Concentrations De Contraintes page 45
- [12] Combustion and heat calculation of an incinerator, E. R. KAISER, Department of Chemical Engineering New York University,pg.81

LIST OF FIGURE

Figure 1: STRESS AMPLITUDE IN FUNCTION OF NUMBER OF CYCLES.....	10
Figure 2:FATIGUE STRENGHT IN FUNCTION OF TENSILE STRENGHT.....	11
Figure 3: CALCULTION OF S_u AND S_{fl} FROM THE VURVE	12
Figure 4: SURFACE FACTOR IN FUNCTION OF THE ULTIMATE STENGHT.....	13
Figure 5: FATIGUE LIMIT IN FUNCTION OF THE ULTIMATE STRENGHT	13
Figure 6: NOMINAL STRESS AND FATIGUE LIFE	16
Figure 7: THE SENSITIVITY FACTOR IN FUNCTION OF RADIUS.....	16
Figure 8: ALTERNATING STRESS IN FUNCTION OF MEAN STRESS.....	17
Figure 9: MULTIAXIAL FATIGUE CRITERIA AND THEIR CLASSIFICATION	19
Figure 10: RANKINE CYCLE AND HIRN CYCLE	22
Figure 11: RANKINE CYCLE MODELISATION IN THERMOPTIM	22
Figure 12: VALUES OF TEMPERATURE AND PRESSURE OBTAINES BY THERMOPTIM	23
Figure 13:THE FREE AND OPEN SOURCE TOOLS USED IN THE STUDY.....	25
Figure 14: THE FORMAT OF FILES	26
Figure 15: A-, D- and O-type boiler configurations.1.Burner; 2.Steam drum; 3.mud drum	27
Figure 16: DESIGN IN FREECAD	27
Figure 17:SHEMATIC OF BOILER	27
Figure 18: THE VAPORIZER IN FREECAD.....	28
Figure 19: Calculation of thickness via browser (chosen material is steel 316L)	29
Figure 20: Calculation of thickness via browser (chosen material is steel 304L)	30
Figure 21: Design of Drum in FreeCAD	30
Figure 22: Group of all parts of a power plant in FreeCAD (boiler, drum, turbine, and condenser).....	31
Figure 23: Design for of the incineration thermal power plant on a real ground using sketch-up (100 m ×100 m)	32
Figure 24: User Interface of Gmsh	34
Figure 25: Mesh of the incinerator CAD model in Gmsh	34
Figure 26: Mesh of the drum CAD model in Gmsh	35
Figure 27: Mesh of the combustion chamber CAD model in Gmsh	35
Figure 28: Convergence history window in ElmerSolver.	36
Figure 29: Imported meshed Vaporizer and steam drum in Elmer	37
Figure 30: DISPLACEMENT IN THE X DEIRECTION.....	38
Figure 31: DISPLACMENT IN THE Y DIRECTION.....	39
Figure 32: DISPLACEMENT IN THE Z DIRECTION	40
Figure 33: STRESS Y_Y	41
Figure 34: STRESS Z_Z	41
Figure 35: STRESS X_X	42
Figure 36: STRESS X_Y	43
Figure 37: STRESS Y_Z	43
Figure 38: STRESS X_Z	44
Figure 39: STRESS X_X IN THE DRUM.....	45
Figure 40:STRESS X_Z IN THE TUBE.....	46
Figure 41: THE STRES IN THE X_Y DIRECTION IN FUNCTION OF THE TIME	48
Figure 42: THE STRES IN THE X DIRECTION IN FUNCTION OF THE TIME	48

Figure 43: THE STRES IN THE Y DIRECTION IN FUNCTION OF THE TIME.....	48
Figure 44: THE STRES IN THE XYDIRECTION IN FUNCTION OF THE STRESS IN THE X DIRECTION.....	48
Figure 45: THE STRES IN THE XY DIRECTION IN FUNCTION OF THE STRESS IN THE X DIRECTION.....	49
Figure 46: THE STRES IN THE XYDIRECTION IN FUNCTION OF THE STRESS IN THE Y DIRECTION.....	49
Figure 47: THE CUMULATIVE PERCENT FAILURES IN FUNCTION OF FATIGUE LIFE	51
Figure 48: THE HYSTHERESIS LOOP.....	52
Figure 49: SMITH-WATSON-TOPPER MODEL.....	53
Figure 50: FATEMI-SOCIE MODEL IN THE PLANE A0.....	54
Figure 51: FATEMI-SOCIE MODEL IN THE PLANE B45.....	54
Figure 52: FATEMI-SOCIE MODEL IN THE PLANE A54.....	55
Figure 59: Results of Fallo software.....	57
Figure 60. BETA DISTRIBUTION	58
Figure 61: WIEBULL DISTRIBUTION.....	58
Figure 62: LOD-NORM DISTRIBUTION	59
Figure 63: Results of FALIN software	59
Figure 64: FATIGUE DATA	60
Figure 65: CYCLIC CURVE	60

LIST OF TABLE

Table 1: THE VALUES OF A AND BETTA.....	14
Table 2: THE VALUES OF KI.....	14
Table 3: Results obtained using THERMOPTIM	24
Table 4: MECHANICAL CONSTANT OF THE STAINLESS STEEL 304L.....	47
Table 5: CALCULATION OF THE SAFETY FACTOR	49
Table 6: <i>Probabilistic analysis of the number of fatigue cycles.</i>	50

GLOSSARY

Alternating Stress (S_a): The alternating stress, S_a , is the amount the stress deviates from the mean. It is sometimes called the stress amplitude.

Endurance Limit (S_{FL}): Steel specimens tested in the laboratory exhibit a safe stress below which failure will not occur. This safe stress is called the endurance limit or the fatigue limit. This behavior is only found in steel. In aluminum alloys, fatigue strength at 10^7 cycles is usually used in place of the fatigue limit. This is a stress which will produce failures in 10^7 cycles.

Fatigue Limit (SFL): Steel specimens tested in the laboratory exhibit a safe stress below which failure will not occur. This safe stress is called the endurance limit or the fatigue limit. This behavior is only found in steel. In aluminum alloys, fatigue strength at 107 cycles is usually used in place of the fatigue limit. This is a stress which will produce failures in 107 cycles.

Fatigue Notch Factor (K_f): Experiments have shown that the effect of small notches is less than that estimated from the traditional stress concentration factor, K_t . The fatigue notch factor, K_f , can be thought of as the effective stress concentration in fatigue. It depends on the size of the stress concentration and the material. Small stress concentrations are more effective in high strength materials. This effect is dealt with using a notch sensitivity factor, q . $K_f = 1 + (K_t - 1)q$. The notch sensitivity factor q is an empirically determined constant that depends on the notch radius and material strength.

Fatigue Strength (S_{FL}): The stress required to produce failures in a specified number of cycles. In steel this is usually 10^6 cycles and is 10^7 cycles for welds and aluminum alloys. It is directly related to the strength of the material.

Loading Factor (k_L): Historically, fatigue limits have been determined from simple bending tests where there is a stress gradient in the test specimen. A specimen loaded in tension will have a lower fatigue limit than one loaded in bending. An empirical correction factor, called the loading factor, is used to make an allowance for this effect.

Mean Stress (S_m): The mean stress, S_m , is the average value of the stresses.

Safety Factor: The safety factor is how much you want to underestimate the maximum strength of the materials in order to ensure a safe design. A single safety factor is applied to both the stress amplitude and the mean stress.

Size Factor (k_{size}): Experimentally, larger parts have lower fatigue limits than smaller parts. Since the materials data is obtained from small specimens, a correction factor, called the size factor, is used for larger diameters. For non-circular sections an effective diameter is computed. The effective diameter is obtained by equating the volume of material subjected to 95% of the maximum stress to a round bar in bending with the same highly stressed volume.

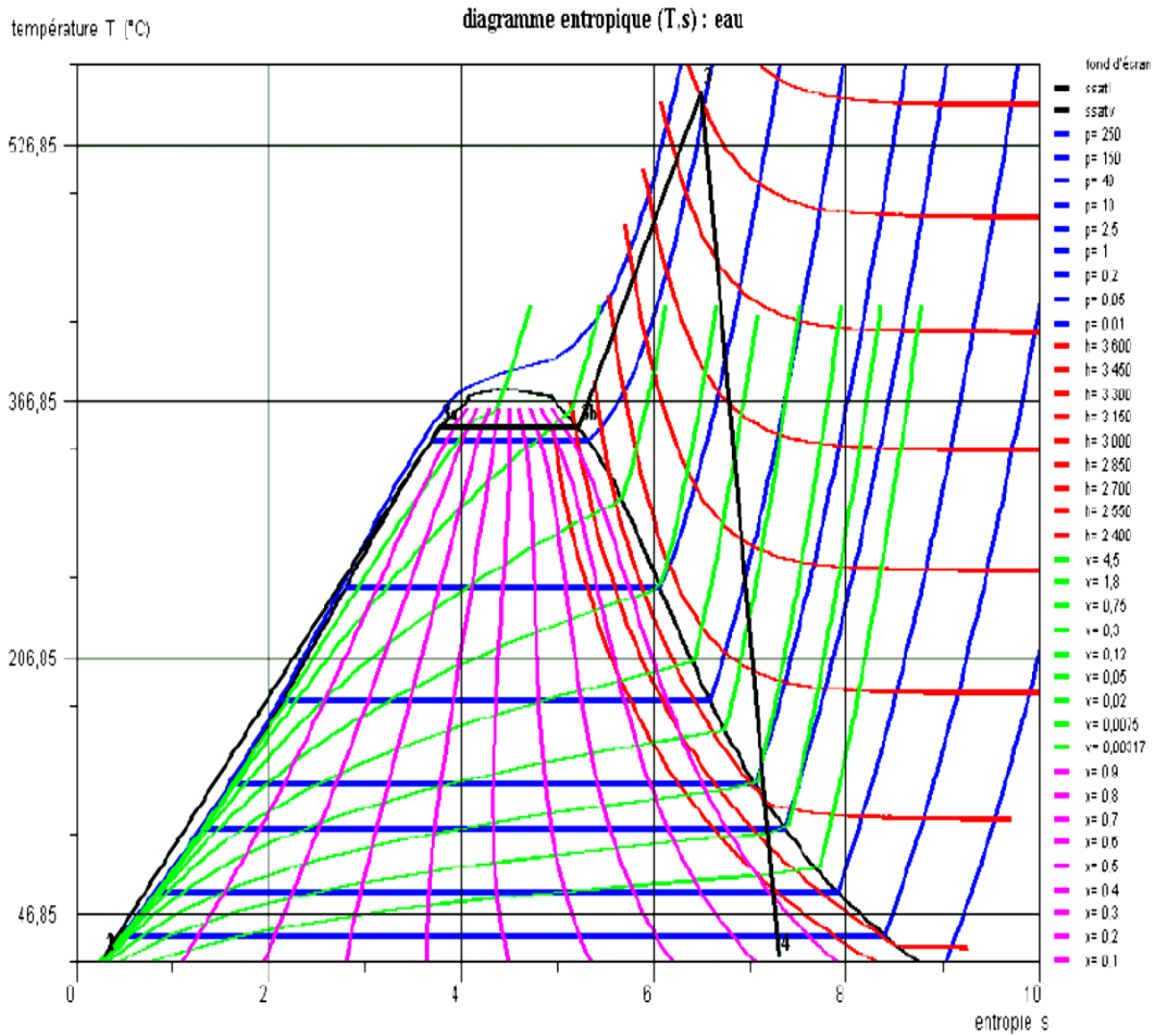
Stress Amplitude (S_a): The stress amplitude, S_a , is the amount the stress deviates from the mean. It is sometimes called the alternating stress.

Stress Concentration Factor (K_t): Stress concentrations arise from any abrupt change in the geometry of a part under load. As a result, the stress distribution is not uniform throughout the cross-section.

Ultimate Strength (S_u): The ultimate strength, S_u , is also called the tensile strength. It is the maximum stress reached in an engineering stress strain diagram.

Annex

1. Annex 1: Water steam Diagram



2. Annex 2: Task of master thesis



Ras Nhache/Batroun - Tripoli, 11th Jan 2015

TEMO-IPP Incineration Demonstration Plant Ras Nhache/Batroun, Lebanon

Vaporizer of TEMO-IPP incineration demonstration plant at Ras Nhache/Batroun



Stress distribution (FEM Analysis) at vaporizer



Upscaled vaporizer train element (TEMO-IPP has to be upscaled in such a way) (picture is from Dr.-Ing. M. Franz, "Dampferzeuger", www.axpo-holz.ch/Dampferzeuger.pdf)

Master Thesis

Mechanical Analysis of an upscaled version of the Vaporizer (pressure vessel and circulation tubes) of the incineration pilot power plant TEMO-IPP

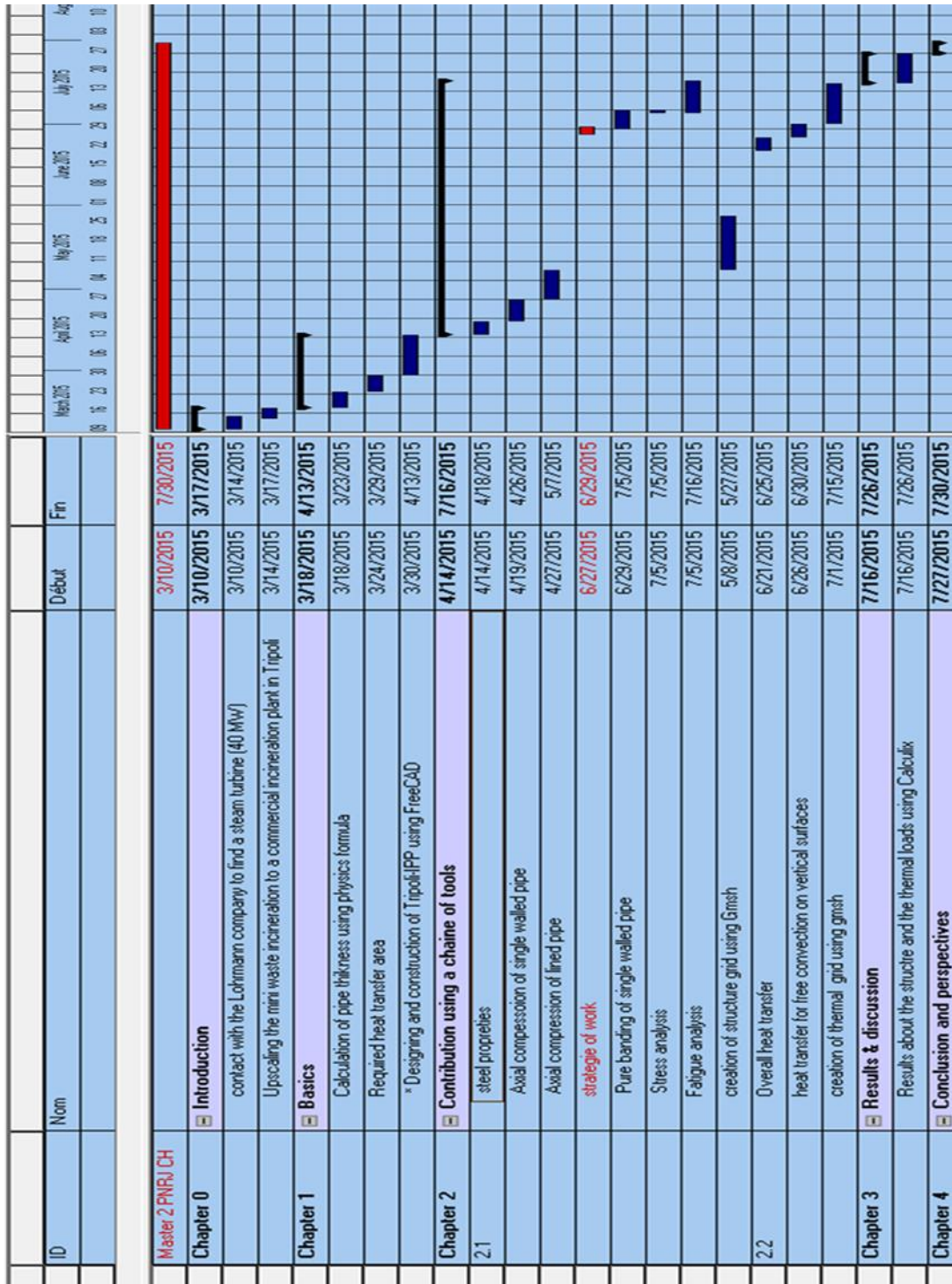
To be able to upscale the TEMO-IPP incineration plant to a commercial incineration plant in Tripoli (about 40 MW) critical components shall be verified by Finite Element Analysis with the tool Abaqus. The main critical component is the pressure vessel with about 100 bar pressure difference. Working packages:

- Upscaling the CAD model of vaporizer with CAD tool ProE (2 weeks)
- Mechanical Behavior (Stress Analysis, Fatigue Analysis, Thermal Strain Analysis) with the tool Abaqus (6 weeks)
- Thermal Loads (Dimensionless Numbers, Overall Heat Transfer, Heat Transfer for Concentric Annular Gaps, Heat Transfer for Free Convection on Vertical Surfaces) with the tool Abaqus (4 weeks)
- Documentation (3 weeks)

Keywords: Alternative Energy, Incineration Power Plant, Mechanical Analysis, Finite Element Analysis (FEA), CAD

Contact: Samir Mourad, Email: samir.mourad@aecenar.com

3. Annex 3: Time plan



4. Appendix 4: The properties of the steam at the inlet of the turbine

POWER PLANTS
OIL REFINERIES
SALE & RELOCATION



Taunusstr. 5a Tel. +49 (0) 611-50402-0 www.lohrmann.com
65183 Wiesbaden/Germany Fax +49 (0) 611-50402-50 info@lohrmann.com

For Sale:	Pre-owned 30.2 MW Steam Turbine Generator Extraction – Condensing Type
Ref.-No:	STG-29.33

Brief plant history:

The steam turbine generator was part of a combined cycle power plant commissioned in 1996 and shut down 2012 after approx. 86,562 operating hours.

Description of major plant components:

Turbine

Manufacturer, Type	ABB Turbinen Nürnberg GmbH, VEE 40 Double extraction condensing turbine, Type 4 Stages HP, 9 stages MP and 9 stages LP part
Max. terminal power	30.2 MW
Number of extractions/ bleeders	1 pcs / 2 pcs.
Live steam parameters	120 bar, 520 °C, 210 t/h
Bleeding 1 normal/max.	36 / 41 bar, 365 / 415 °C, max. 80 t/h
Bleeding 2 normal/max.	6 / 8.5 bar, 170 / 333 °C, max. 75 t/h
Extraction normal/max.	16 / 20.5 bar, 275 / 300 °C, max. 20 t/h
Exhaust normal/max.	0.047 / 0.08 bar, max. 18 °C
Rate max.	10.2 / 55.6 t/h

Budget Price for STG 29.33: FOB 3.150.000 EUR (Offer from 12 Oct 2015)

6. Annex 6: Physical properties of stainless steel 316L (Reference Materials Engineering-Mechanical Behavior Report 128)

Material Type	stainless steel
Material Specification	AISI 316
Material Alloy	30316
Elastic Modulus	$E = 190000 \text{ MPa}$
Crack Growth Intercept	$C = 4.26\text{E-}13 \text{ m/cycle}$
Crack Growth Exponent	$m = 3.6$
Threshold Stress Intensity	$\Delta K_{TH} = 5.15 \text{ MPa sqrt (m)}$
Ultimate Strength	$S_u = 650 \text{ MPa}$
Fatigue Strength Coefficient	$\sigma' = 1000 \text{ MPa}$
Fatigue Strength Exponent	$b = -0.114$
Fatigue Ductility Coefficient	$\epsilon' = 0.171$
Fatigue Ductility Exponent	$c = -0.402$
Cyclic Strength Coefficient	$K' = 1660 \text{ MPa}$
Cyclic Strain Hardening Exponent	$n' = 0.287$
Curve Intercept	$S_f' = 924 \text{ MPa}$
Curve Slope	$b = -0.114$
Fracture Strenght	650 MPa
Fracture strain	1.73
Poisson ration	0.25